Supporting Information

Multifunctional stimuli-responsive chemogenetic platform for conditional multicolor cell-selective labeling

Pengfei Chen, Rui Wang, Ke Wang, Jiao-Na Han, Shi Kuang, Zhou Nie* and Yan Huang*

State Key Laboratory of Chemo/Biosensing and Chemometrics, College of Chemistry and Chemical Engineering, Hunan Provincial Key Laboratory of Biomacromolecular Chemical Biology, Hunan University, Changsha, 410082 (P. R. China)

*E-mail：niezhou.hnu@gmail.com, yanhuang@hnu.edu.cn

Table of Contents

1. Synthesis and Characterization

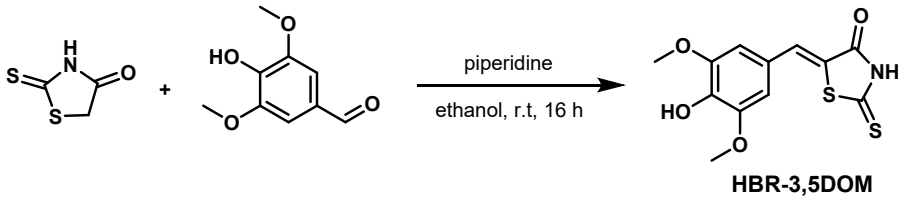

Synthesis of (Z)-5-(4-Hydroxy-3,5-dimethoxybenzylidene)-2-thioxothiazolidin-4-one (HBR-3,5DOM).

To a stirred solution of rhodanine (200 mg, 1.5 mmol, 1.0 eq.) and 4-hydroxy-3,5-dimethoxybenzaldehyde (285 mg, 1.56 mmol, 1.1 eq.) in 4.5 mL of absolute ethanol, piperidine (140 μL, 1.5 mmol, 1.0 eq.) was added and then stirred at room temperature for 16 h. After the reaction, the solution was neutralized by an aqueous solution of HCl. Subsequently, cooling to 4 °C and standing for 2 h, the precipitate was filtered and dried.

^{1}H NMR (400 MHz, DMSO-d_6) δ 13.73 (s, 1H), 9.49 (s, 1H),7.60 (s, 1H), 6.91 (s, 2H), 3.85 (s, 6H).

^{13}C NMR (101 MHz, DMSO-d_6) δ 195.83, 169.83, 148.77, 139.62, 133.52, 123.68, 121.90, 108.91, 56.54.

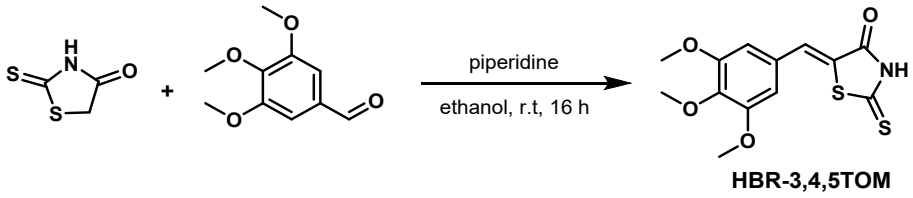

Synthesis of (Z)-2-thioxo-5-(3,4,5-trimethoxybenzylidene)thiazolidin-4-one (HBR-3,4,5TOM).

To a stirred solution of rhodanine (200 mg, 1.5 mmol, 1.0 eq.) and 3,4,5-trimethoxybenzaldehyde (306 mg, 1.56 mmol, 1.1 eq.) in 4.5 mL of absolute ethanol, piperidine (140 μL, 1.5 mmol, 1.0 eq.) was added and then stirred at room temperature for 16 h. After the reaction, the solution was neutralized by an aqueous

solution of HCl. Subsequently, cooling to 4 °C and standing for 2 h, the precipitate was filtered and dried.

^{1}H NMR (400 MHz, DMSO- d_6) δ 7.58 (s, 1H), 6.88 (s, 2H), 3.84 (s, 6H), 3.74 (s, 3H).

^{13}C NMR (101 MHz, DMSO-d_6) δ 195.92, 169.74, 153.71, 140.20, 132.51, 128.89, 124.76, 108.38, 60.70, 56.48.

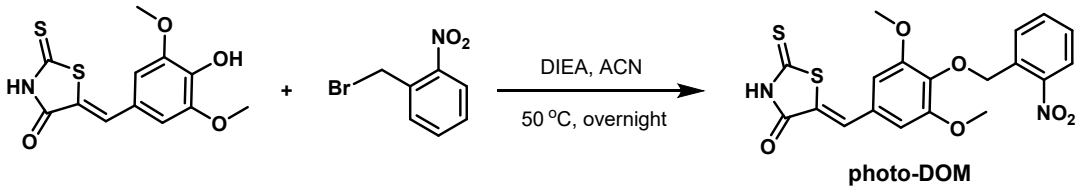

Synthesis of (Z)-5-(3,5-dimethoxy-4-((2-nitrobenzyl)oxy)benzylidene)-2-thioxothiazolidin-4-one (photo-DOM).

A solution containing HBR-3,5DOM (37 mg, 0.125 mmol, 1.0 eq.) and 1-(bromomethyl)-2-nitrobenzene (32 mg, 0.15 mmol, 1.2 eq.) in 20 mL of acetonitrile (ACN) was stirred at room temperature, and then 50 μL (0.25 mmol, 2.0 eq.) N,N-Diisopropylethylamine (DIEA) was added and stirred at 50 °C for 12 h. When the reaction was completed, the solvent was removed by rotary evaporation. The crude product was purified by thin-layer chromatography (CH_2Cl_2: EtOH = 120: 1, v/v) to afford photo-DOM.

^{1}H NMR (400 MHz, DMSO-d_6) 9.56 (s, 1H), 8.16 (d, J = 8.4 Hz, 1H), 7.89-7.79 (m, 3H), 7.69-7.63 (m, 1H), 6.98 (s, 2H), 5.01 (s, 2H), 3.85 (s, 6H).

^{13}C NMR (101 MHz, DMSO-d_6) δ 190.71, 179.19, 148.76, 148.37, 140.22, 137.68, 134.84, 133.31, 131.66, 130.24, 125.75, 123.79, 122.54, 108.97, 56.55, 54.74.

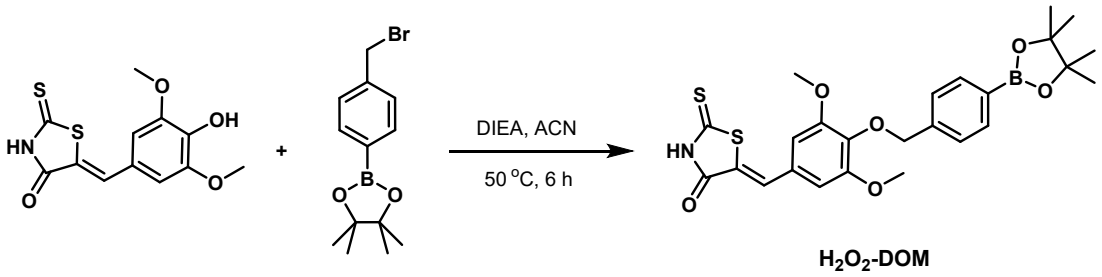

Synthesis of (Z)-5-(3,5-dimethoxy-4-((4-(4,4,5,5-tetramethyl-1,3,2-dioxaborolan-2-yl)benzyl)oxy)benzylidene)-2-thioxothiazolidin-4-one (H_2O_2-DOM).

A solution containing HBR-3,5DOM (74 mg, 0.25 mmol, 1.0 eq.) and 2-(4-(bromomethyl)phenyl)-4,4,5,5-tetramethyl-1,3,2-dioxaborolane (111 mg, 0.375 mmol, 1.5 eq.) in 40 mL of acetonitrile was stirred at room temperature, and then 100 μL (0.5 mmol, 2.0 eq.) DIEA was added and stirred at 50 °C for 6 h. When the reaction was completed, the solvent was removed by rotary evaporation. The crude product was purified by thin-layer chromatography (CH_2Cl_2: toluene: EtOH = 50: 2: 1, v/v/v) to afford H_2O_2-DOM.

^{1}H NMR (400 MHz, DMSO-d_6) δ 9.56 (s, 1H),7.83 (s, 1H), 7.70 (d, J = 7.7 Hz, 2H), 7.54 (d, J = 7.7 Hz, 2H), 6.98 (s, 2H), 4.77 (s, 2H), 3.86 (s, 6H), 1.32 (s, 12H).

^{13}C NMR (101 MHz, DMSO-d_6) δ 190.79, 179.46, 148.76, 139.85, 137.21, 135.21, 129.12, 128.68, 123.82, 122.63, 84.21, 56.56, 25.11.

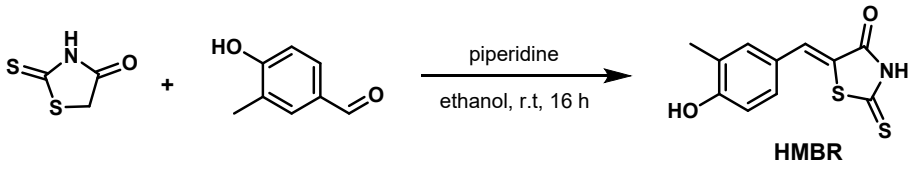

Synthesis of (Z)-5-(4-hydroxy-3-methylbenzylidene)-2-thioxothiazolidin-4-one (HMBR).

To a stirred solution of rhodanine (200 mg, 1.5 mmol, 1.0 eq.) and 4-hydroxy-3-methylbenzaldehyde (213 mg, 1.56 mmol, 1.1 eq.) in 4.5 mL of absolute ethanol, piperidine (140 μL, 1.5 mmol, 1.0 eq.) was added and then stirred at room temperature for 16 h. After the reaction, the solution was neutralized by an aqueous

solution of HCl. Subsequently, cooling to 4 °C and standing for 2 h, the precipitate was filtered and dried.

^{1}H NMR (400 MHz, DMSO-d_6) δ 13.70 (s, 1H), 10.39 (s, 1H), 7.53 (s, 1H), 7.41-7.25 (m, 2H), 6.95 (d, J = 8.3 Hz, 1H), 2.18 (s, 3H).

^{13}C NMR (101 MHz, DMSO-d_6) δ 196.02, 169.95, 159.18, 134.11, 133.15, 131.09, 125.99, 124.29, 121.07, 116.07, 16.34.

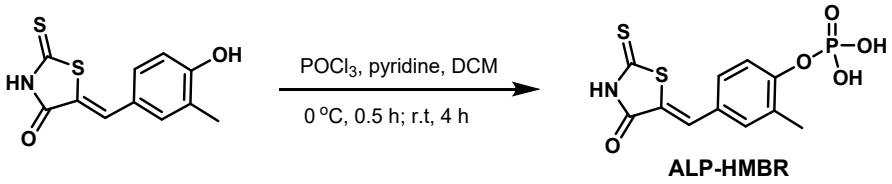

Synthesis of (Z)-2-methyl-4-((4-oxo-2-thioxothiazolidin-5-ylidene)methyl)phenyl dihydrogen phosphate (ALP-HMBR).

HMBR (126 mg, 0.5 mmol, 1 eq.) was dissolved in 4 mL anhydrous pyridine and 6 mL dichloromethane, and $POCl_3$ (140 uL, 1.5 mmol, 3 eq.) was then added under ice bath. After stirring at room temperature for 4 h, 200 mL of ice water was added and stirred overnight. The precipitate was filtered under pressure and dried in vacuums to afford ALP-HMBR.

^{1}H NMR (400 MHz, D_2O) δ 7.30 (s, 1H), 7.26-7.18 (m, 2H), 6.53 (d, J = 8.5 Hz, 1H), 2.02 (s, 3H).

^{31}P NMR (162 MHz, D_2O): δ - 4.49.

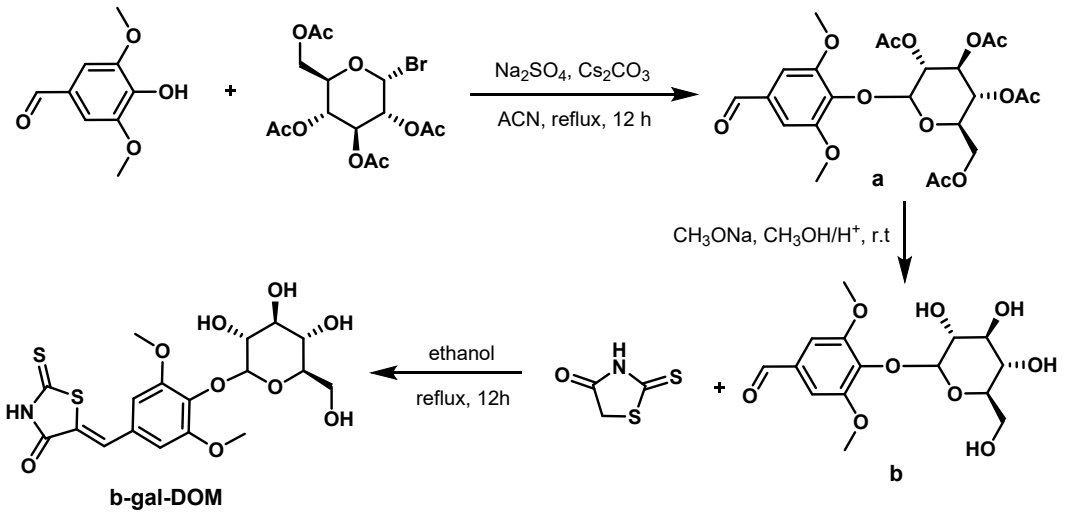

Synthesis of 5-((Z)-3,5-dimethoxy-4-(((3R,4S,5S,6R)-3,4,5-trihydroxy-6-(hydroxymethyl)tetrahydro-2H-pyran-2-yl)oxy)benzylidene)-2-thioxothiazolidin-4-one (β-gal-DOM).

To a stirred solution of 4-hydroxy-3,5-dimethoxybenzaldehyde (1.09g, 6 mmol, 1 eq.) in 50 mL of acetonitrile, Na_2SO_4 (2.13 g, 15 mmol, 2.5 eq.) and Cs_2CO_3 (4.89 g, 15 mmol, 2.5 eq.) were added. Subsequently, 2,3,4,6-Tetra-O-acetyl-α-D-glucopyranosyl bromide was added and refluxed for 12 h. After cooling to room temperature, the solvent was removed by rotary evaporation. The crude product was purified by silica gel column chromatography (PE: EtOAc = 1: 1, v/v) to afford compound a.

Compound a (2.0581 g, 5 mmol) was dissolved in 21 mL methanol and 9 mL dichloromethane, and 30% sodium methanolate in methanol (4 mL, 20 mmol) was added and stirred at room temperature for 4 h. After neutralization with Amberlite IR-120 (H), the mixture was filtered and concentrated under vacuum. The crude product was purified by column silica gel chromatography (CH_2Cl_2: CH_3OH = 10: 1, v/v) to obtain compound b as a white solid.

A mixture of compound b (68.8 mg, 0.2 mmol, 1 eq.) and rhodanine (40 mg, 0.3 mmol, 1.5 eq.) in 25 mL solvent (15 mL ethanol + 10 mL methanol) was refluxed at 80 °C for 12 h. After the reaction, the solvent was removed by rotary evaporation. The crude product was purified by thin-layer chromatography (CH_2Cl_2: CH_3OH: EtOH = 10: 1: 1, v/v/v) to afford β-gal-DOM.

2. Experimental Section

2.1 Materials and Instruments

All the chemical reagents were purchased from commercial suppliers (Bide Pharmatech or Energy Chemical) and used without further purification, unless otherwise stated. Alkaline phosphatase and β-galactosidase were purchased from Sangon Biotech (Shanghai, China). DMEM medium was obtained from Neuronbc (Beijing, China), and fetal bovine serum (FBS) was obtained from Biological Industries USA. Penicillin-Streptomycin (100×) and 0.25% Trypsin-EDTA were supplied by NCM Biotech (Suzhou, China). Mito-Tracker Green and DiI (1,1'-dioctadecyl-3,3,3',3'-tetramethylindocarbocyanine perchlorate) were purchased from Beyotime (China). Lipofectamine™ 8000 transfection reagent was obtained from Thermo Fisher Scientific (USA). All the stock solutions of the synthetic ligands were prepared in DMSO with a concentration of 10 mM and stored at -20 ℃ except for ALP-HMBR. ALP-HMBR was dissolved in 50 mM Tris-HCl buffer (pH = 7.4) with a concentration of 200 μM and stored at -20 ℃. Ultrapure water obtained from a Millipore water purification system (≥ 18 MΩ, Milli-Q, Millipore, Billerica, MA) was used in all runs.

Thin-layer chromatography analysis was performed on silica gel plates, and column chromatography was conducted by silica gel (mesh 200-300) columns. ^{1}H NMR spectra were recorded at 400 MHz on a Bruker-400 spectrometer with tetramethylsilane (TMS) as the internal standard. Mass spectra were performed using Bruker FT-ICR MS (9.4T). UV-vis absorption spectra were performed on a UV-vis spectrophotometer (Agilent). Fluorescence measurements were recorded on a Photon Technology International (PTI) QM40 fluorescence spectrophotometer (HORIBA) or Synergy™ Mx multi-mode microplate reader (BioTek, USA). Flow cytometry was carried out with a flow cytometer (Becton Dickinson), and imaging was performed on a confocal laser scanning microscope (CLSM) (Nikon, Eclipse TE2000-E, Japan) or inverted microscope (Leica DMi8, Germany). UV LED lamp (λ =365 nm) was used

for photoactivation. pH measurements were carried out on a Mettler-Toledo Delta 320 pH meter.

2.2 Plasmid construction, protein expression and purification

pET28a-*fast*, pcDNA3.1-*fast*, pcDNA3.1-*mito-fast* and pcDNA3.1-*mem-fast* were constructed from Sangon Biotech. The gene of NLS-sfGFP and FSAT were amplified by PCR using Q5 High-Fidelity DNA Polymerase and customized specific primers, and then inserted into pcDNA3.1 via Xba I/Hind III restriction sites to build the construct pcDNA3.1-*nls-gfp-fast*.

nucleotide sequence of fast

ATGGAGCATGTTGCCTTTGGCAGTGAGGACATCGAGAACACTCTGGCCA
AAATGGACGACGGACAACTGGATGGGTTGGCCTTTGGCGCAATTCAGCTC
GATGGTGACGGGAATATCCTGCAGTACAATGCTGCTGAAGGAGACATCAC
AGGCAGAGATCCCAAACAGGTGATTGGGAAGAACTTCTTCAAGGATGTTG
CACCTGGAACGGATTCTCCCGAGTTTTACGGCAAATTCAAGGAAGGCGTA
GCGTCAGGGAATCTGAACACCATGTTCGAATGGATGATACCGACAAGCAG
GGGACCAACCAAGGTCAAGGTGCACATGAAGAAAGCCCTTTCCGGTGAC
AGCTATTGGGTCTTTGTGAAACGGGTAGGT

nucleotide sequence of mito-fast

ATGTCCGTCCTGACGCCGCTGCTGCTGCGGGGCTTGACAGGCTCGGCCC
GGCGGCTCCCAGTGCCGCGCGCCAAGATCCATTCGTTGGGATCCATGGAG
CATGTTGCCTTTGGCAGTGAGGACATCGAGAACACTCTGGCCAAAATGGA
CGACGGACAACTGGATGGGTTGGCCTTTGGCGCAATTCAGCTCGATGGTG
ACGGGAATATCCTGCAGTACAATGCTGCTGAAGGAGACATCACAGGCAG
AGATCCCAAACAGGTGATTGGGAAGAACTTCTTCAAGGATGTTGCACCTG
GAACGGATTCTCCCGAGTTTTACGGCAAATTCAAGGAAGGCGTAGCGTCA
GGGAATCTGAACACCATGTTCGAATGGATGATACCGACAAGCAGGGGAC
CAACCAAGGTCAAGGTGCACATGAAGAAAGCCCTTTCCGGTGACAGCTAT
TGGGTCTTTGTGAAACGGGTAGGT

nucleotide sequence of mem-fast

ATGCTGTGCTGCATGCGTCGTACCAAACAGGTGGAAAAAAATGATGAT
GATCAGAAAATTCCGGTCGCCACCATGGAGCATGTTGCCTTTGGCAGTGA
GGACATCGAGAACACTCTGGCCAAAATGGACGACGGACAACTGGATGGG
TTGGCCTTTGGCGCAATTCAGCTCGATGGTGACGGGAATATCCTGCAGTA
CAATGCTGCTGAAGGAGACATCACAGGCAGAGATCCCAAACAGGTGATT
GGGAAGAACTTCTTCAAGGATGTTGCACCTGGAACGGATTCTCCCGAGTT
TTACGGCAAATTCAAGGAAGGCGTAGCGTCAGGGAATCTGAACACCATGT
TCGAATGGATGATACCGACAAGCAGGGGACCAACCAAGGTCAAGGTGCA
CATGAAGAAAGCCCTTTCCGGTGACAGCTATTGGGTCTTTGTGAAACGGG
TAGGT

nucleotide sequence of nls-gfp-fast

CCAAAAAAGAAGAGAAAGGTAGATCCAAAAAAGAAGAGAAAGGTAGA
TCCAAAAAAGAAGAGAAAGGTACCGGTCGCCACCATGCGCAAAGGAGAA
GAACTTTTCACTGGAGTTGTCCCAATTCTTATTGAATTAGATGGTGATGTT
AATGGGCACAAATTTTTTGTCCGTGGAGAGGGTGAAGGTGATGCTACAAT
CGGAAAACTCAGCCTTAAATTTATTTGCACTACTGGAAAACTACCTGTTCC
ATGGCCAACACTTGTCACTACTCTGACCTATGGTGTTCAATGCTTTTCCCG
TTATCCGGATCACATGAAACGGCATGACTTTTTCAAGAGTGCCATGCCCG
AAGGTTATGTACAGGAACGCACTATATATTTCAAAGATGACGGGACCTAC
AAGACGCGTGCTGAAGTCAAGTTTGAAGGTGATACCCTTGTTAATCGTAT
CGAGTTAAAAGGTATTGATTTTAAAGAAGATGGAAACATTCTCGGACACA
AACTCGAGTACAACTTTAACTCACACAAAGTATACATCACGGCAGACAAA
CAAAATAATGGAATCAAAGCTAACTTCACAATTCGCCACAACGTTGAAGA
TGGTTCCGTTCAACTAGCAGACCATTATCAACAAAATACTCCAATTGGCG
ATGGCCCTGTCCTTTTACCAGACAACCATTACCTGTCGACACAAACTGTCC
TTTCGAAAGATCCCAACGAAAAGCGTGACCACATGGTCCTTCATGAGTCT
GTAAATGCTGCTGGGATTACACATGGCATGGATGAGCTCTACAAAGGTGG
TGGTTCTggatccATGGAGCATGTTGCCTTTGGCAGTGAGGACATCGAGAAC
ACTCTGGCCAAAATGGACGACGGACAACTGGATGGGTTGGCCTTTGGCGC

AATTCAGCTCGATGGTGACGGGAATATCCTGCAGTACAATGCTGCTGAAG
GAGACATCACAGGCAGAGATCCCAAACAGGTGATTGGGAAGAACTTCTTC
AAGGATGTTGCACCTGGAACGGATTCTCCCGAGTTTTACGGCAAATTCAA
GGAAGGCGTAGCGTCAGGGAATCTGAACACCATGTTCGAATGGATGATAC
CGACAAGCAGGGGACCAACCAAGGTCAAGGTGCACATGAAGAAAGCCCT
TTCCGGTGACAGCTATTGGGTCTTTGTGAAACGGGTAGGT

The construct pET28a-*fast* was transformed into *E. coli* BL21 (DE3) by heat shock. Cells were then incubated in Lysogeny Broth (LB) medium at 37 °C for 2 h until an OD_{600} of 0.6-0.8 was reached, and then were induced with 1 mM isopropyl β-D-1-thiogalactopyranoside (IPTG) at 37 °C for 4 h. Cells were harvested by centrifugation (8000 rpm for 15 min at 4 °C) and re-suspended in lysis buffer (phosphate buffer 50 mM, NaCl 150 mM, $MgCl_2$ 2.5 mM, pH 7.4), and lysed by sonication on ice for 40 min. Cellular fragments were removed by centrifugation (10000 rpm for 20 min at 4 °C). Protein in the supernatant was purified by Ni-NTA agarose chromatography (ÄKTA, GE) and then the buffer was exchanged into 50 mM phosphate buffer (pH 7.4) containing 150 mM NaCl by desalination chromatography (ÄKTA, GE). The expression level and purity of the protein were investigated using SDS-PAGE. The purified FAST was quantified by BCA Protein Assay Kit, and was stored at -20°C.

2.3 Calculation of the relative fluorescence quantum yield.

The relative fluorescence quantum yield was calculated using the Equation S1,

$$\Phi_{f(X)} = \Phi_{f(S)} (n_X/n_S)^2 A_S F_X/(A_X F_S) \qquad (S1)$$

where Φ_f is the relative fluorescence quantum yield; A is the absorbance at the excitation wavelength; F is the area under the corrected emission curve, and n is the refractive index of the solvent. Subscripts S and X refer to the standard and the unknown, respectively. The solutions of HBR-3,5DOM, HBR-3,4,5TOM, their respective complex with FAST and the standard rhodamine 6G were kept absorptions below 0.05.

2.4 Affinity measurements

The dissociation constant (K_d) for the FAST:ligand complex was calculated by

measuring the fluorescence decrease as a function of the increasing concentration of the caged-ligand in the presence of 5 μM HBR-3,5DOM and 0.5 μM FAST. K_d value was obtained by non-linear regression fitting to the data using equation S2.

$$y = \frac{ymax}{1 + 0.196 * (1 + \frac{x}{K2})} \quad \text{(S2)}$$

This equation is derived from the chemical equilibrium reaction as shown below:

1) $P + L \rightleftharpoons PL$

2) $P + I \rightleftharpoons PI$

$$K_1 = \frac{[P] * [L]}{[PL]}$$

$$K_2 = \frac{[P] * [I]}{[PI]} = \frac{\frac{K1 * [PL]}{[L]} * [I]}{[P0] - [P] - [PL]} = \frac{\frac{K1 * [PL]}{[L]} * [I]}{[P0] - \frac{K1 * [PL]}{[L]} - [PL]} =$$

$$\frac{\frac{K1}{[L]} * [I]}{\frac{[P0]}{[PL]} - \frac{K1}{[L]} - 1}$$

where P represents protein (FAST), L represents ligand (HBR-3,5DOM) and I represents inhibitor (caged-ligand). K_1 is defined as the dissociation constant of ligand, K_2 is the dissociation constant of inhibitor.

When $[L_0] >> [P_0]$, $[L] \approx [L_0]$, $[I] \approx x$, $[P_0] \approx a*y_{max}$, $[PL] \approx a*y$;

$$K_2 = \frac{\frac{K1}{[L0]} * x}{\frac{ymax}{y} - \frac{K1}{[L0]} - 1}$$

$$y = \frac{ymax}{1 + \frac{K1}{[L0]} * (1 + \frac{x}{K2})}$$

According to report in the literature[3], the dissociation constant of FAST and HBR-3,5DOM is 0.98 μM. So, in this experiment, K_1 = 0.98 μM, $[L_0]$ = 5 μM:

$$y = \frac{ymax}{1 + 0.196 * (1 + \frac{x}{K2})}$$

where y represents the measured fluorescence intensity, y_{max} is the initial fluorescence intensity of FAST:HBR-3,5DOM, and x is the concentration of the caged-ligand. Final data analysis was conducted using Origin 2021 (OriginLab Corp.).

2.5 Response assay of srFAST *in vitro*

For photo-srFAST responding to light, photo-DOM (5 μM) and FAST (5 μM) were mixed in PBS buffer (50 mM phosphate, 150 mM NaCl, pH 7.4). The solution was irradiated with UV LED lamp for different times (0, 2, 4, 6, 8, 10, 12, 14, 16 min). The fluorescence spectra of the solution were recorded using Synergy™ Mx multi-mode microplate reader, before and after UV irradiation.

For H_2O_2-srFAST responding to H_2O_2, H_2O_2-DOM (5 μM) and FAST (2.5 μM) were mixed in PBS buffer (50 mM phosphate, 150 mM NaCl, pH 7.4). Then H_2O_2 with different concentrations (0-1 mM) was added to the solution and reacted at 37°C for 2 h. Finally, the fluorescence spectra of the solutions were recorded using Synergy™ Mx multi-mode microplate reader.

For ALP-srFAST responding to ALP, ALP-HMBR (5 μM) and FAST (5 μM) were mixed in Tris-HCl buffer (50 mM, pH 7.4). Then ALP with different concentrations (0-300 U/L) was added to the solution, and reacted at 37°C for 90 min. Similarly, for β-gal-srFAST responding to β-gal, β-gal-DOM (5 μM) and FAST (5 μM) were mixed in PBS buffer (50 mM phosphate, 150 mM NaCl, pH 7.4). Then β-gal with different concentrations (0-1.3 U/mL) was added to the solution and reacted at 37°C for 60 min.

Finally, the fluorescence spectra of the solutions were detected using Synergy™ Mx multi-mode microplate reader.

2.6 Cell culture

All cells were cultured with high glucose DMEM containing 10% FBS, 100 U/mL penicillin and 100 μg/mL streptomycin in an incubator (Thermo Scientific) at 37 °C under an atmosphere of 5 % CO_2 and 90 % relative humidity.

2.7 Plasmid transfection

Cells were seeded in the confocal dish or 96-well plates and cultured at 37 °C for 1 day before transfection. Then the plasmid was transiently transfected using Lipofectamine™ 8000 transfection reagent according to the manufacturer's protocols for 24 h to express the corresponding protein.

2.8 Co-culture of different cell types

Ibidi μ-Dish $^{35\ mm,high}$ and Culture-Insert 3 Well were used for co-culturing of 2 or 3 types of cells. The cells transfected with the corresponding construct for 24 h were seeded in each well and then incubated at 37 °C and 5 % CO_2 for 24 h. After appropriate ce attachment, the Culture-Insert 3 Well was removed by using sterilized twlleezer. Subsequently, the dish was washed slightly and treated with H_2O_2-DOM, HBR-3,5DOM, ALP-HMBR and β-gal-DOM, or HMBR and HBR-3,5DOM before cell imaging.

2.9 Cell imaging

To examine the performance of photo-srFAST, HEK293T cells expressing NLS-sfGFP-FAST were incubated in PBS, photo-DOM (5 μM) or HBR-3,5DOM (5 μM) for 30 min respectively, and then the cells were illuminated without or with UV LED lamp for 10 min. For time-dependent imaging, the same cells were illuminated with UV for 0, 2, 4, 6, 8 and 10 min accumulatively. Cell imaging experiments were performed on a confocal laser scanning microscope (CLSM) (Nikon, Eclipse TE2000-E) with a 60× oil immersion objective at room temperature. sfGFP: E_x/E_m 488/500-550 nm; photo-DOM, HBR-3,5DOM: E_x/E_m 561/570-620 nm.

For the spatiotemporal imaging of nucleus, HEK293T cells expressing NLS-sfGFP-FAST were incubated with 5 μM photo-DOM for 30 min, then the cells at specific area were exposed to the irradiation of 405 nm (laser, 40 mW/cm^2) sequentially. Cell imaging was performed on an inverted microscope (Leica, DMi8) with a 20 × or 63× oil immersion objective. sfGFP: E_x/E_m 484/505-550 nm; photo-DOM: E_x/E_m 510/560-620 nm.

To examine the performance of H_2O_2-srFAST, HEK293T cells expressing mito-FAST were incubated in PBS containing H_2O_2-DOM (2.5 μM) or H_2O_2 (200 μM) and H_2O_2-DOM (2.5 μM) for 2 h, respectively, after staining the mitochondria with 200 nM Mito-Tracker Green following the product instruction. For imaging during respiratory burst, RAW 264.7 cells or HEK293T cells expressing mito-FAST were pre-treated with 2 μg/mL PMA for 40 min after staining with 200 nM Mito-Tracker Green, and then incubated in PBS containing H_2O_2-DOM (2.5 μM) or HBR-3,5DOM (2.5 μM) for 2 h. Cell imaging experiments were performed on a confocal laser scanning microscope (CLSM) (Nikon, Eclipse TE2000-E) with a 60× oil immersion objective at room temperature. Mito-Tracker Green: E_x/E_m 488/500-550 nm; H_2O_2-DOM, HBR-3,5DOM: E_x/E_m 561/570-620 nm.

For imaging of the co-cultured RAW 264.7 and HEK293T cells under PMA stimulation, the cells were treated with 2 μg/mL PMA for 40 min, and then incubated with H_2O_2-DOM (2.5 μM) or HBR-3,5DOM (2.5 μM) for 2 h. Cell imaging was performed on an inverted microscope (Leica, DMi8) with a 10× dry objective and a 63× oil immersion objective. H_2O_2-DOM, HBR-3,5DOM: E_x/E_m 510/560-620 nm.

To examine the performance of ALP-srFAST, HeLa cells expressing mem-FAST were incubated with 5 μM ALP-HMBR for 90 min, after staining the cell membrane with 5 μM DiI following the product instruction. For inhibition analysis, HeLa cells were pre-treated with 400 μM Na_3VO_4 for 30min, and then incubated with 5 μM ALP-HMBR for 90 min, after staining the cell membrane with 5 μM DiI. To examine the performance of β-gal-srFAST, SKOV-3 cells expressing mem-FAST were incubated with 5 μM HMBR + 5 μM β-gal-DOM for 90 min. For inhibition analysis,

SKOV-3 cells were pre-treated with 1 mM D-galactose for 30 min before being incubated with HMBR and β-gal-DOM. For imaging of specific cancer cells, HeLa and SKOV-3 cells both expressing mem-FAST were incubated with the same solution (5 μM HBR-3,5DOM, 5 μM ALP-HMBR + 5 μM HBR-3,5DOM, 5 μM HMBR, 5 μM HMBR + 5 μM β-gal-DOM or 5 μM HMBR + 5 μM HBR-3,5DOM, respectively). Cell imaging was performed on a confocal laser scanning microscope (CLSM) (Nikon, Eclipse TE2000-E) with a 60× oil immersion objective at room temperature. ALP-HMBR, HMBR: E_x/E_m 488/500-550 nm; β-gal-DOM, HBR-3,5DOM: E_x/E_m 561/570-620 nm; DiI: E_x/E_m 561/570-620 nm.

For multicolor selective imaging of the co-cultured cells, HeLa, HEK293T and SKOV-3 cells were treated with a mixture of ALP-HMBR (5 μM) and β-gal-DOM (5 μM) or a mixture of HMBR (5 μM) and HBR-3,5DOM (5 μM) for 90 min, respectively. Imaging was performed on an inverted microscope (Leica, DMi8) with a 10× dry objective and a 63× oil immersion objective. ALP-HMBR, HMBR: E_x/E_m 440/505-550 nm; β-gal-DOM, HBR-3,5DOM: E_x/E_m 510 nm/560-620 nm.

All images were processed and analyzed using ImageJ.

2.10 Cytotoxicity assay

Cytotoxicity of the synthetic ligands was evaluated by CCK8 assay. In a 96-well plate, 100 μL cell-containing solution with the cell density of 2×10^4 cells mL^{-1} was added to each well and incubated at 37 °C for 24 h. Then, the cells were treated with different concentrations of ligands (0, 1, 2, 5, 10, 15 and 20 μM for photo-DOM, H_2O_2-DOM and ALP-HMBR; 0, 2, 5, 10, 20, 30 μM for β-gal-DOM) for 6 h, or the cells were treated with 5 μM photo-DOM, H_2O_2-DOM, ALP-HMBR or β-gal-DOM for increasing incubation durations (0, 2, 4, 6, 8, 12, 24 h), respectively. After being washed with PBS, the cells were incubated with a mixture of 10 μL CCK8 and 90 μL DMEM for 4 h. The optical absorbance at 450 nm of the final solution was measured using a microplate reader (Biotek). Cell viability (%) was calculated according to the equation: Viability = (mean Abs. of treated wells/mean Abs. of control wells) × 100%. Each experiment was tested in 5 replicates.

2.11 Flow cytometry

Flow cytometry was used to evaluate the performance of different srFASTs at the group level of cells. Briefly, cells expressing specific FAST were firstly harvested in PBS buffer to prepare cell suspensions, and then 1×10^5 cells were treated with different ligands (10 μM photo-DOM, H_2O_2-DOM, ALP-HMBR or β-gal-DOM) and corresponding conditions in 200 μL buffer for an appropriate time. Subsequently, the cells were suspended before flow cytometry analysis using the flow cytometer (Abcam, USA).

2.12 Theoretical Calculation

To explore the fluorescence properties of HBR-3,5DOM and HBR-3,4,5TOM in water, density functional theory (DFT) was performed using Gaussian 09. The density functional theory calculation with CAM-B3LYP method was applied to the geometry optimization of all molecules in the ground (S_0) and excited state (S_1) with 6-31+G(d) basis set in water. [1,2] The HOMO and LUMO energies at S_0 and S_1 state are calculated from the geometrically optimized molecule.

2.13 Molecular docking

The initial crystal structure for FAST was downloaded from RCSB Protein Data Bank (PYP, PDB: 1NWZ).[3,4] A homology modeling conducted by the SWISS-MODEL (https://swissmodel.expasy.org/) to acquire the best structure of FAST. The optimized structure of HBR-3,4,5TOM is obtained by DFT calculations. Docking of HBR-3,4,5TOM with FAST was performed by AutoDockTools, and then molecular interactions between them were studied by docking simulations via AutoDock 4.2.6. The docking model with the lowest docked free energy was selected for further investigation in this article. All the figures were rendered using the PyMOL Molecular Graphics System (version 2.4.1 Open-Source, Schrödinger, LLC).

3. Supplemental Tables and Figures

3.1 Supplemental Table

Table S1. Physicochemical properties of the FAST:ligand complex in PBS (pH = 7.4).

Compound	Ex (nm)	Em (nm)	ε ($M^{-1}\cdot cm^{-1}$)	Φ_f (%)	Brightness
FAST:HBR-3,5DOM	518	600	39500	32	12640
FAST:HBR-3,4,5TOM	518	595	6500	4.4	286

The abbreviations are as follows: Ex, the wavelength of excitation; Em, the wavelength of emission; ε, the molar absorption coefficient at relative Ex; Φ_f, the relative fluorescence quantum yield; brightness = ε × Φ_f.

3.2 Supplemental Figures

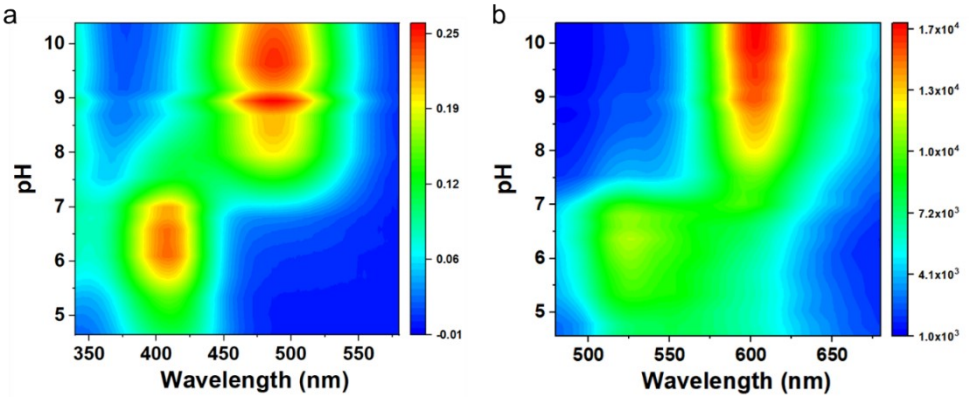

Fig. S1 (a) Absorption spectra and (b) fluorescence emission spectra of HBR-3,5DOM in Britton-Robinson buffer at different pH. λ_{ex} = 518 nm.

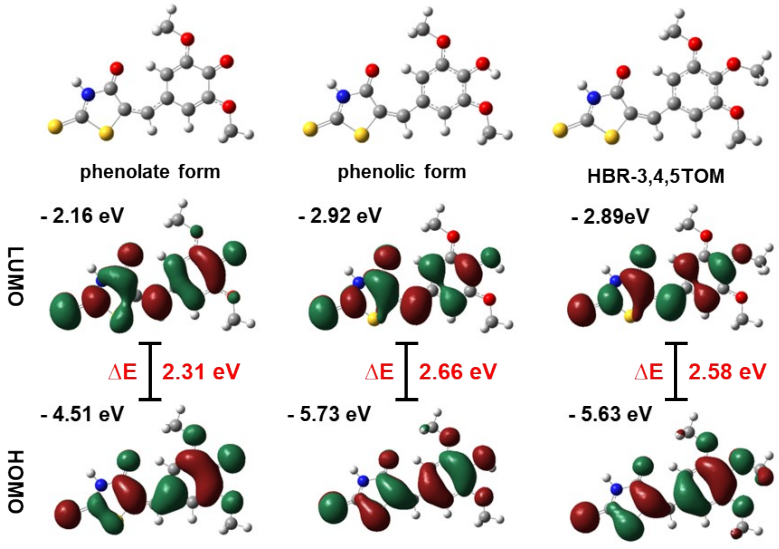

Fig. S2 The optimized structures and molecular orbital plots (HOMO and LUMO) of HBR-3,5DOM and HBR-3,4,5TOM in water (S_1) were calculated by TDDFT.

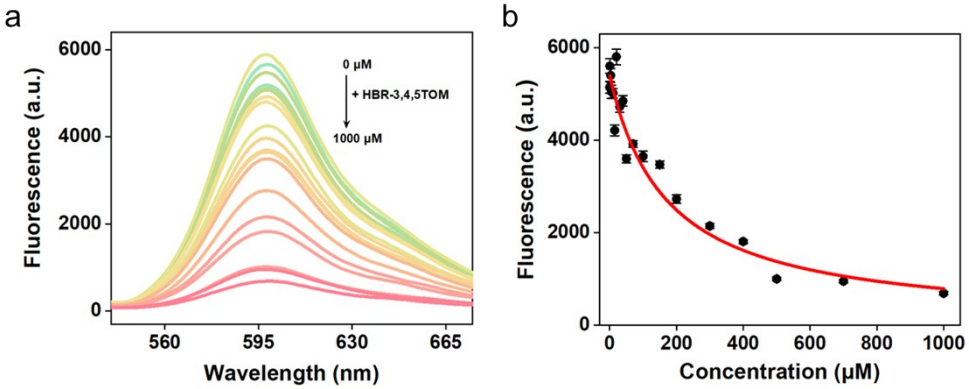

Fig. S3 (a) Fluorescence spectra of the competition assay between HBR-3,4,5TOM and HBR-3,5DOM. Different concentrations of HBR-3,4,5TOM were added to the solution containing 5 μM HBR-3,5DOM and 0.5 μM FAST. (b) The fluorescence intensity at equilibrium for various HBR-3,4,5TOM concentrations in the competition assay. K_d = 28.2 μM. λ_{ex} = 518 nm, λ_{em} = 600 nm.

The competition assay (Fig. S3) depicted that as the HBR-3,4,5TOM concentration increased, the fluorescence of the complex reduced, indicating that HBR-3,4,5TOM can replace HBR-3,5DOM and bind with FAST when the concentration is high enough.

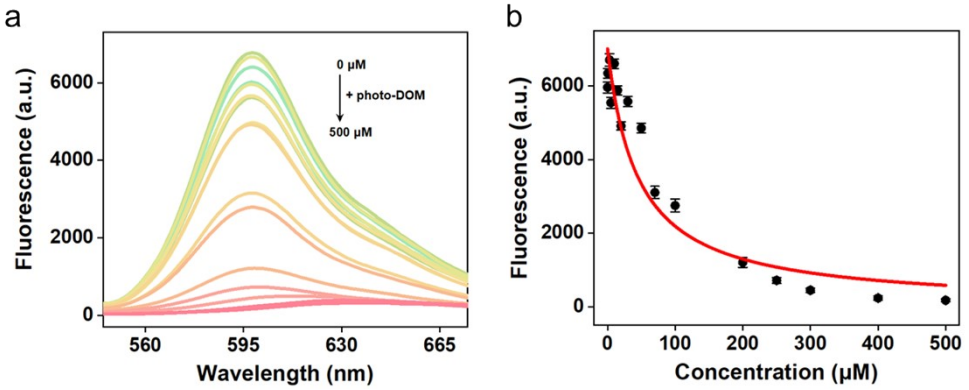

Fig. S4 (a) Fluorescence spectra of the competition assay between photo-DOM and HBR-3,5DOM. Different concentrations of photo-DOM were added to the solution containing 5 μM HBR-3,5DOM and 0.5 μM FAST. (b) The fluorescence intensity at equilibrium for various photo-DOM concentrations in the competition assay. K_d = 7.4 μM. λ_{ex} = 518 nm, λ_{em} = 600 nm.

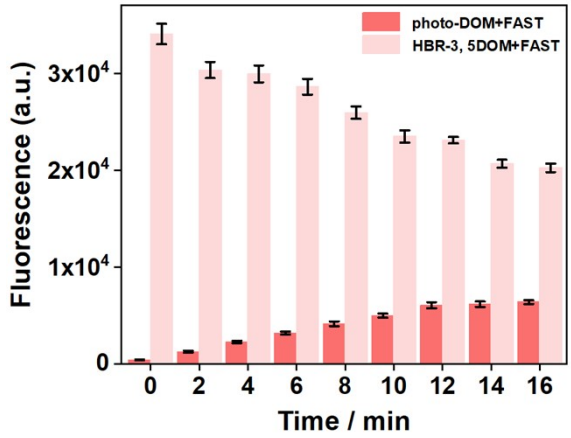

Fig. S5 Fluorescence intensity of the FAST:photo-DOM and the FAST:HBR-3,5DOM complex vs. UV irradiation time respectively (λ_{ex} = 518 nm, λ_{em} = 600 nm). After 12 min irradiation, the fluorescence recovery efficiency of FAST:photo-DOM was 32%.

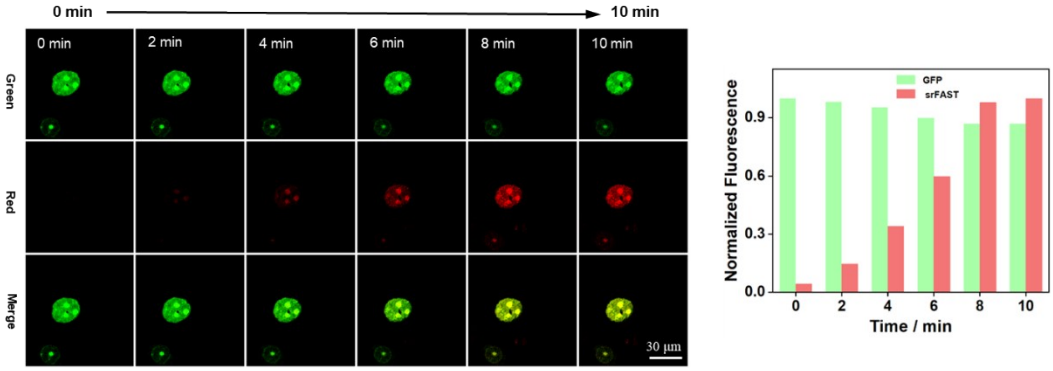

Fig. S6 Irradiation time-dependent fluorescence imaging and quantification of fluorescence intensity of HEK293T cells expressing NLS-sfGPF-FAST, after incubation with 5 μM photo-DOM for 30 min.

Fig S6 shows that the photocaged ligand photo-DOM could be photoactivated continually and then be stable in cells.

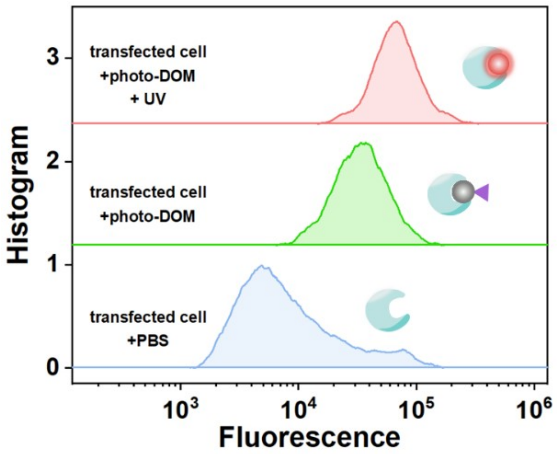

Fig. S7 Flow cytometric analysis of HEK293T cells treated under different conditions.

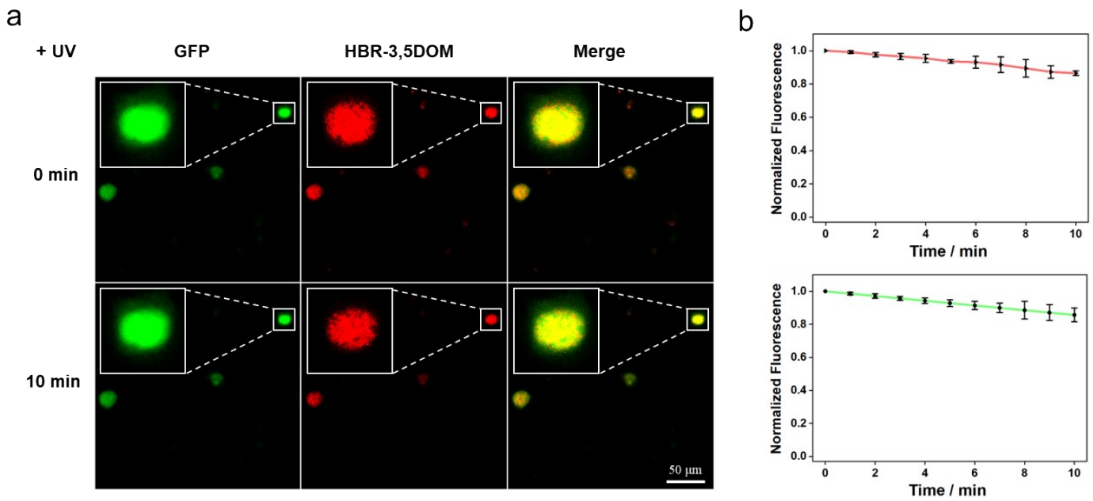

Fig. S8 Photostability of O-FAST after UV irradiation in HEK293T cells. (a) Fluorescence imaging of HEK293T cells expressing NLS-sfGFP-FAST incubated with 5 μM HBR-3,5DOM upon long-term UV irradiation (λ = 365 nm, 3 mW/cm^2). (b) Plots show the fluorescence intensity of sfGFP (green) and O-FAST (red) as a function of UV irradiation time.

These results suggested that there was about 15% photobleaching of the red fluorescence from O-FAST after 10 min UV irradiation in cells.

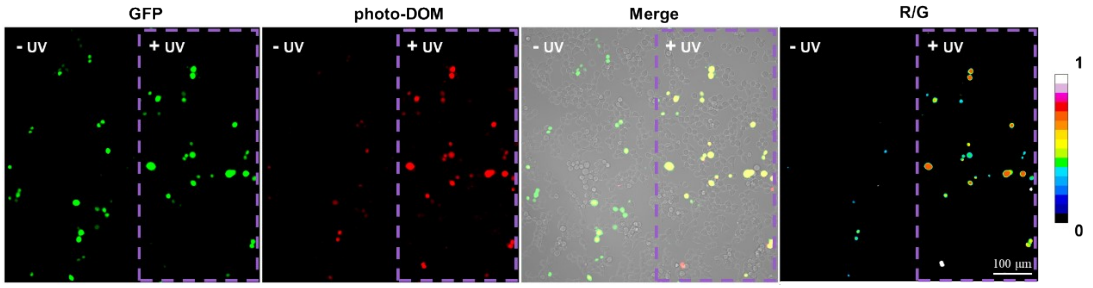

Fig. S9 Spatiotemporal labeling of the nucleus of HEK293T cells in a certain region using photo-srFAST. λ = 405 nm, laser, 40 mW/cm^2.

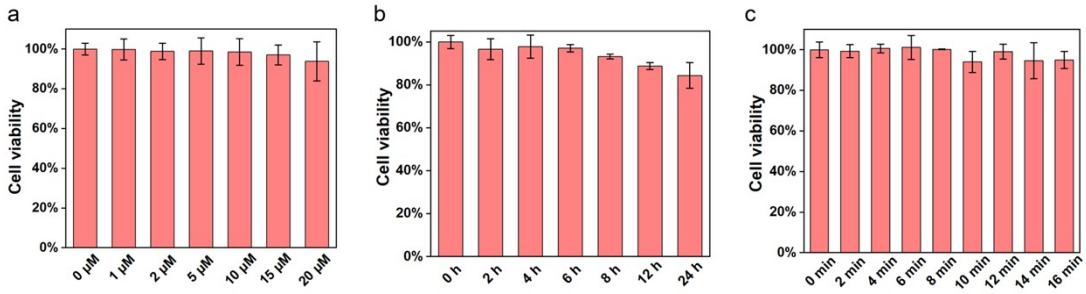

Fig. S10 Cell viability of HEK293T cells measured by CCK8 assay. (a) Effect of the photo-DOM concentration on cell viability. HEK293T cells were incubated with different concentrations of photo-DOM for 6 h. (b) Effect of the incubation time on cell viability after being incubated with 5 μM photo-DOM for different times. (c) Effect of the UV illumination time (3 mW/cm^2) on cell viability.

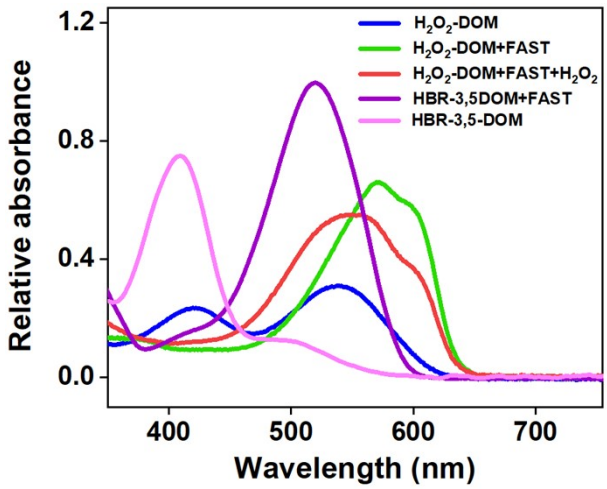

Fig. S11 Absorption spectra of H_2O_2-DOM (blue), the FAST:HBR-3,5DOM complex (purple), the FAST:H_2O_2-DOM complex (green), the FAST:H_2O_2-DOM complex reacted with H_2O_2 for 2 h

(red), and HBR-3,5DOM only (light magenta).

The results showed that the absorption peak of H_2O_2-DOM was red-shifted and the absorption intensity increased after adding FAST protein to the solution, indicating that H_2O_2-DOM can bind with FAST protein. When H_2O_2 was added, the absorption peak was blue-shifted towards that of the FAST:HBR-DOM complex, which suggested that in the presence of H_2O_2, H_2O_2-DOM can remove the boronate group to generate HBR-3,5DOM, thus forming the FAST:HBR-3,5DOM complex.

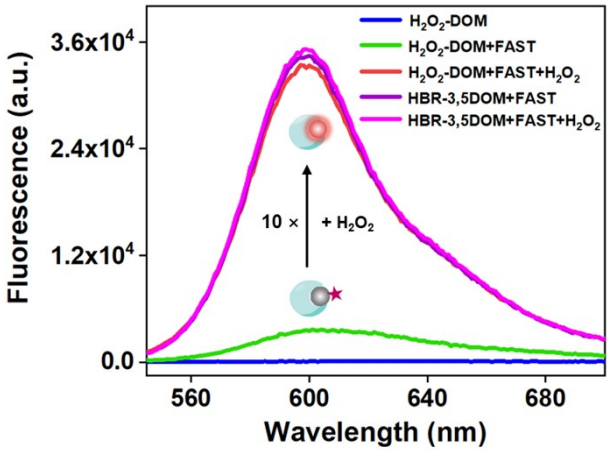

Fig. S12 Fluorescence spectra of H_2O_2-DOM, H_2O_2-DOM + FAST ± H_2O_2 and HBR-3,5DOM + FAST ± H_2O_2. λ_{ex} = 518 nm.

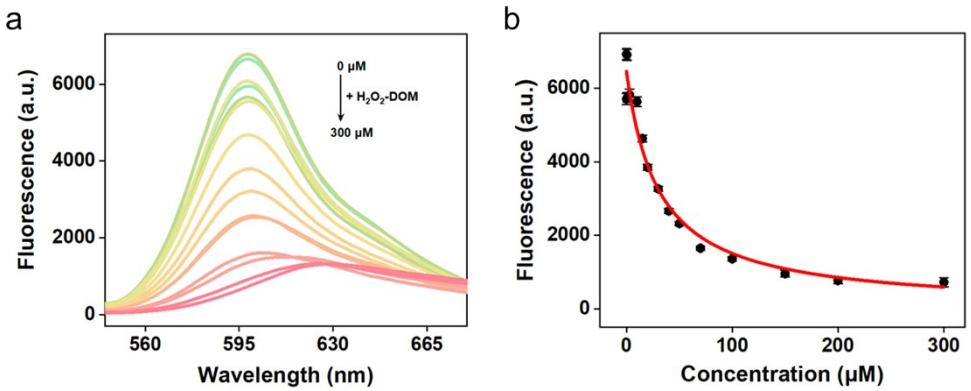

Fig. S13 (a) Fluorescence spectra of the competition assay between H_2O_2-DOM and HBR-3,5DOM. Different concentrations of H_2O_2-DOM were added to the solution containing 5 μM HBR-3,5DOM and 0.5 μM FAST. (b) The fluorescence intensity at equilibrium for various H_2O_2-DOM concentrations in the competition assay. K_d = 5.0 μM. λ_{ex} = 518 nm, λ_{em} = 600 nm.

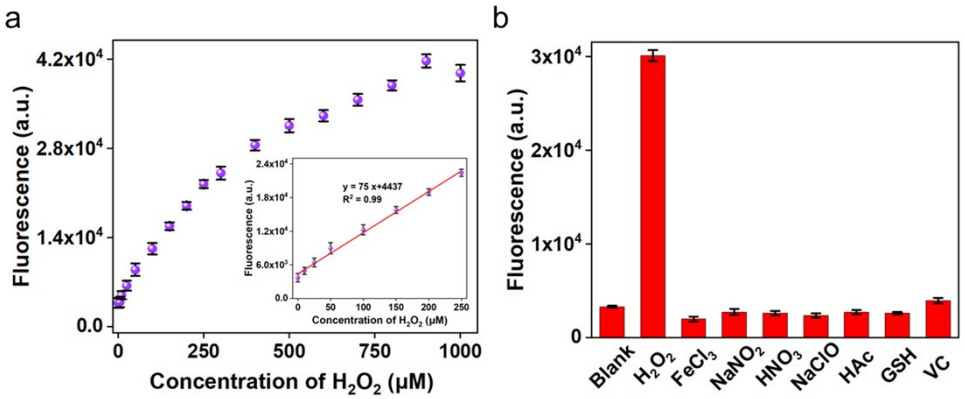

Fig. S14 (a) Fluorescence intensity of the FAST:H_2O_2-DOM complex in the presence of different concentrations of H_2O_2. (b) Fluorescence responses of H_2O_2-srFAST toward different compounds in PBS buffer. The concentration of each compound is 1.0 mM.

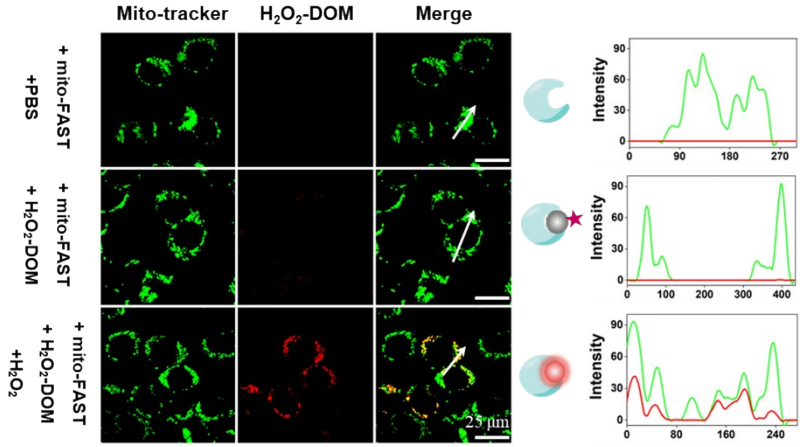

Fig. S15 CLSM images of HEK293T cells transfected with pcDNA3.1-*mito-fast* for 24 h in response to exogenous H_2O_2. The green fluorescence is from the mito-tracker, and the red fluorescence indicates the signal from H_2O_2-srFAST.

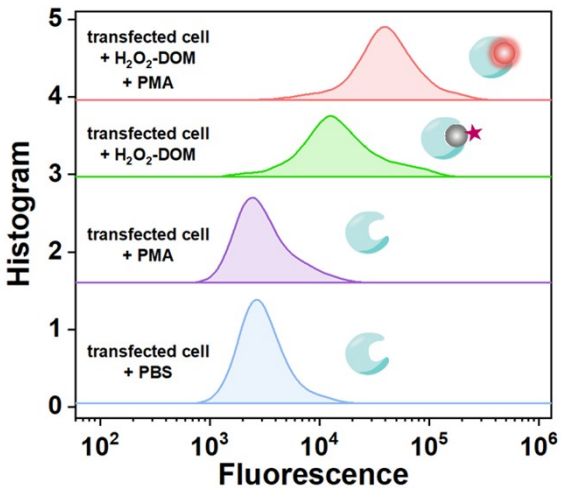

Fig. S16 Flow cytometric analysis of Raw264.7 cells under different conditions.

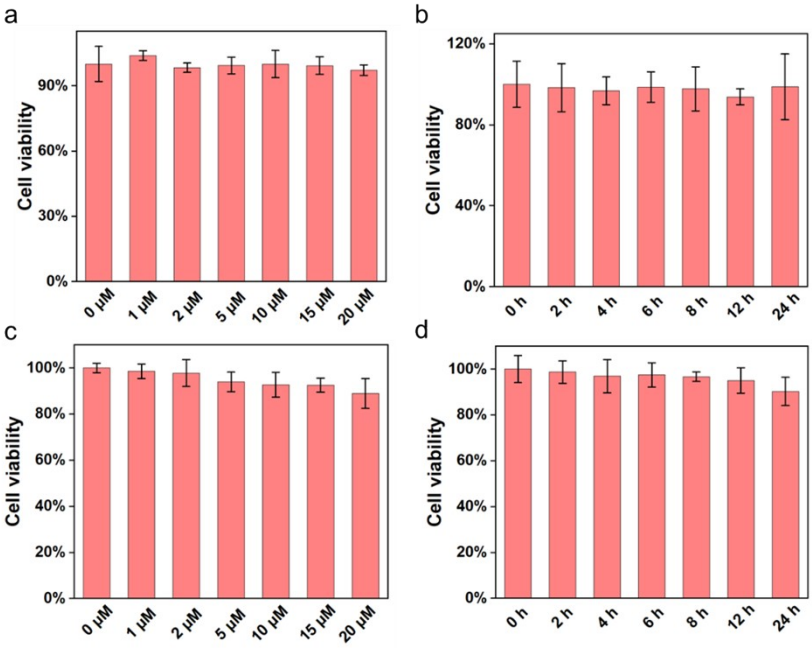

Fig. S17 Cell viability of RAW264.7 (a, b) and HEK293T (c, d) cells measured by CCK8 assay. Effect of the H_2O_2-DOM concentration on viability of (a) RAW264.7 and (c) HEK293T cell. The cells were incubated with different concentrations of H_2O_2-DOM for 6 h. Effect of the incubation time on viability of (b) RAW264.7 and (d) HEK293T cells after being incubated with 5 μM H_2O_2-DOM for different times, respectively.

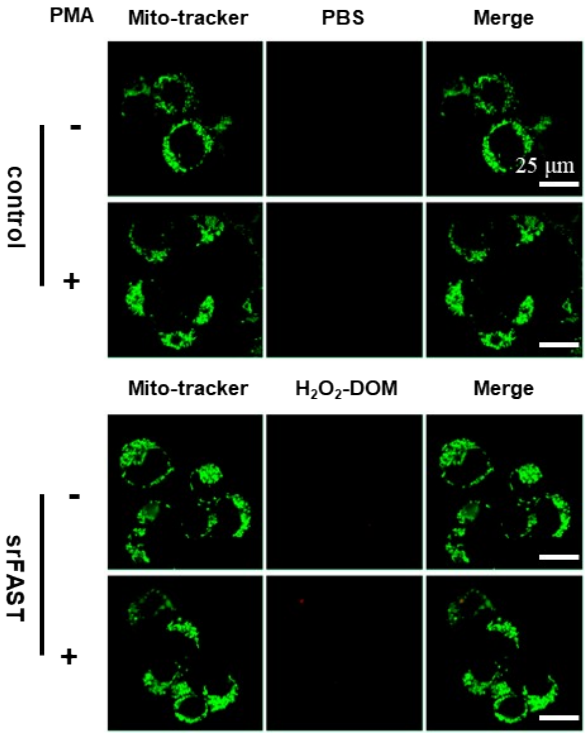

Fig. S18 CLSM images of HEK293T cells transfected with pcDNA3.1-*mito-fast* for 24 h in response to PMA stimulation using H_2O_2-srFAST.

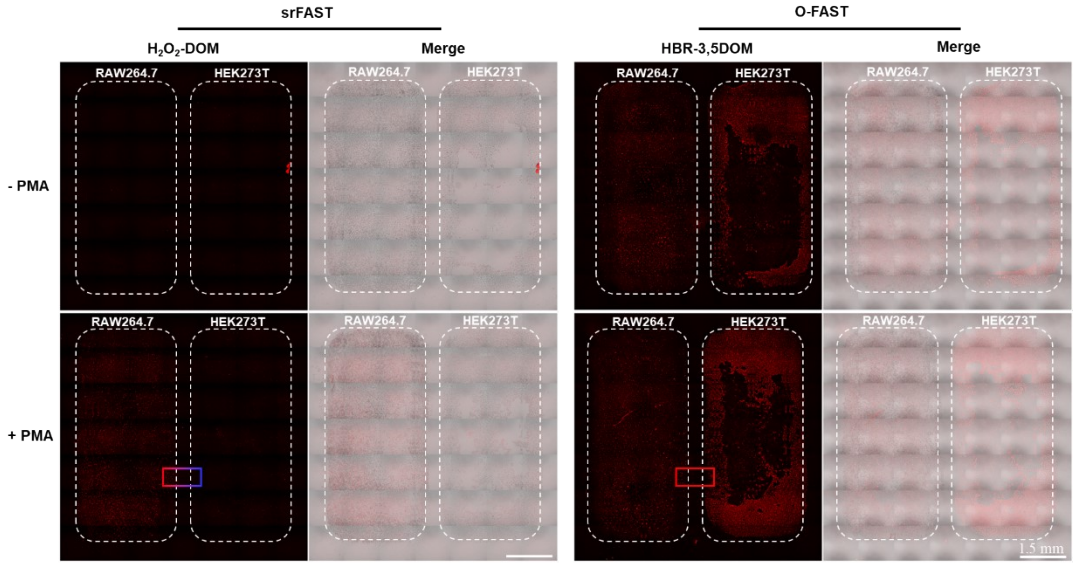

Fig. S19 Application of H_2O_2-srFAST and O-FAST for selective labeling of mitochondria of the co-cultured cells before and after PMA stimulation. Mosaic images of the contiguous fluorescence imaging of corresponding cells throughout the co-culture area.

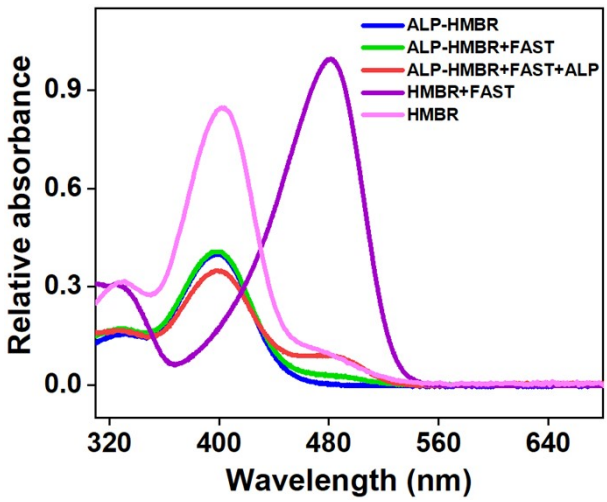

Fig. S20 Absorption spectra of ALP-HMBR (blue), the FAST:ALP-HMBR complex (green), the FAST:ALP-HMBR complex reacted with ALP for 90 min (red), the FAST:HMBR complex (purple), and HMBR only (light magenta).

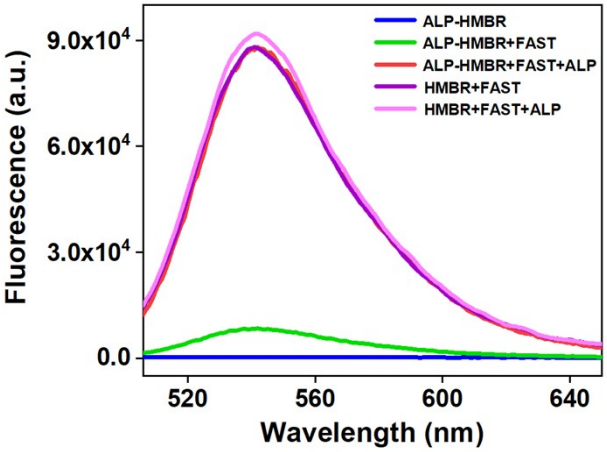

Fig. S21 Fluorescence spectra of ALP-HMBR, ALP-HMBR + FAST ± ALP, and HMBR + FAST ± ALP.

The results of absorption and fluorescence spectra indicate that ALP-HMBR can bind with FAST, and it can also be catalyzed by ALP to generate HMBR, resulting in the FAST:HMBR complex.

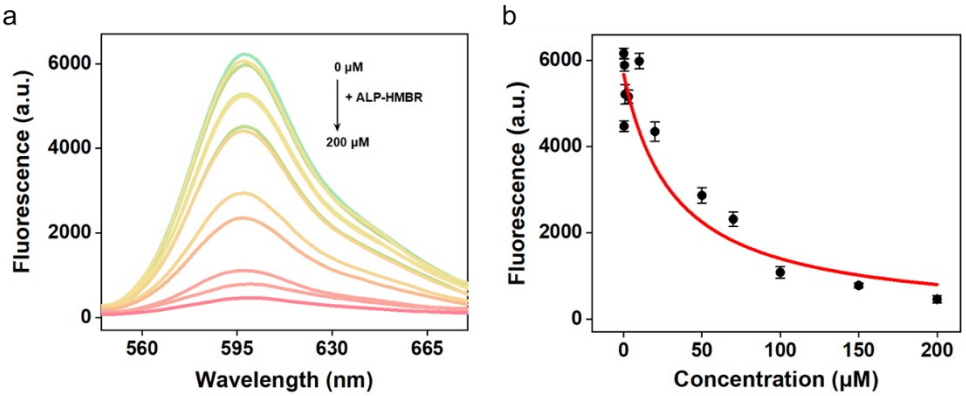

Fig. S22 (a) Fluorescence spectra of the competition assay between ALP-HMBR and HBR-3,5DOM. Different concentrations of ALP-HMBR were added to the solution with 5 μM HMBR-3,5DOM and 0.5 μM FAST. (b) The fluorescence intensity at equilibrium for various ALP-HMBR concentrations in the competition assay. K_d = 5.4 μM. λ_{ex} = 518 nm, λ_{em} = 600 nm.

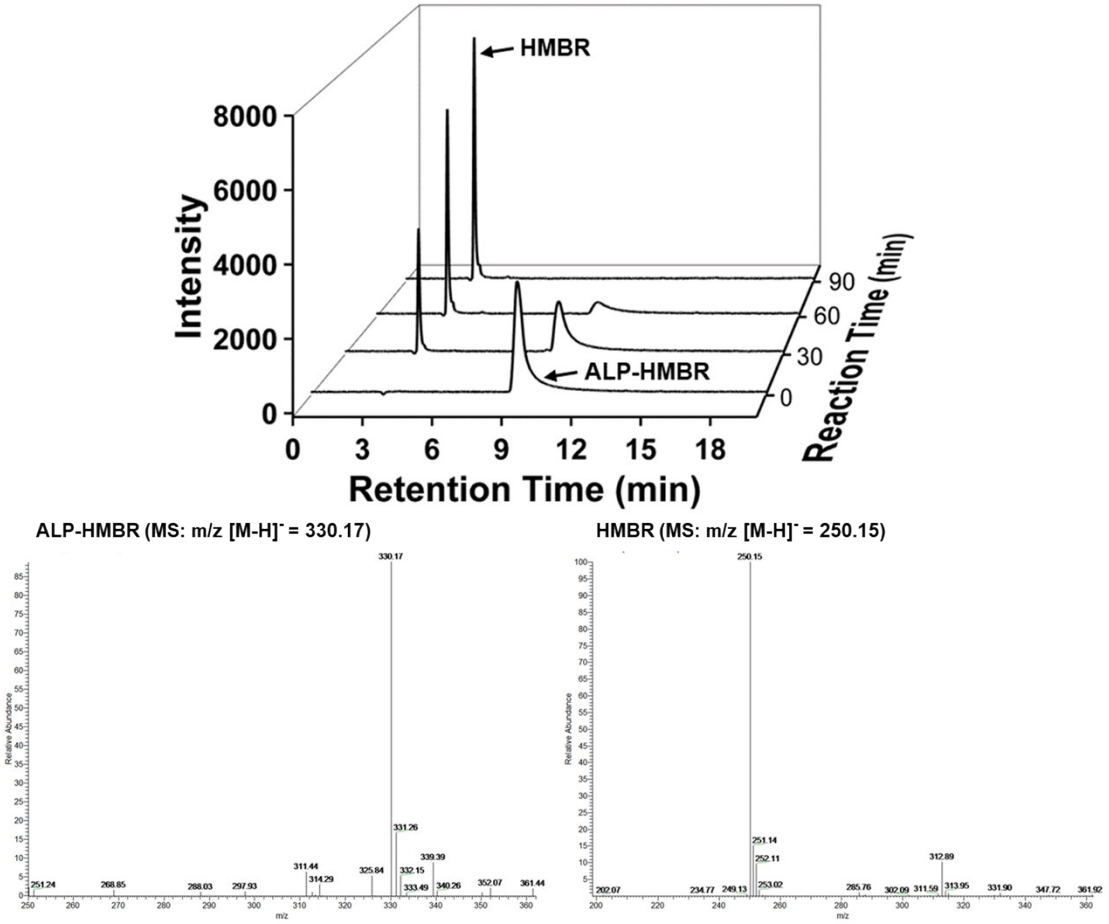

Fig. S23 Time-dependent HPLC [1.0 mL·min^{-1}, MeOH/H_2O (80:20, v/v), 254 nm] and MS of ALP-HMBR after reacting with ALP.

The HPLC and MS results revealed the gradual decrease of ALP-HMBR and the

concomitant increase of HMBR with time, indicating the conversion of ALP-HMBR to HMBR after the enzymatic reaction.

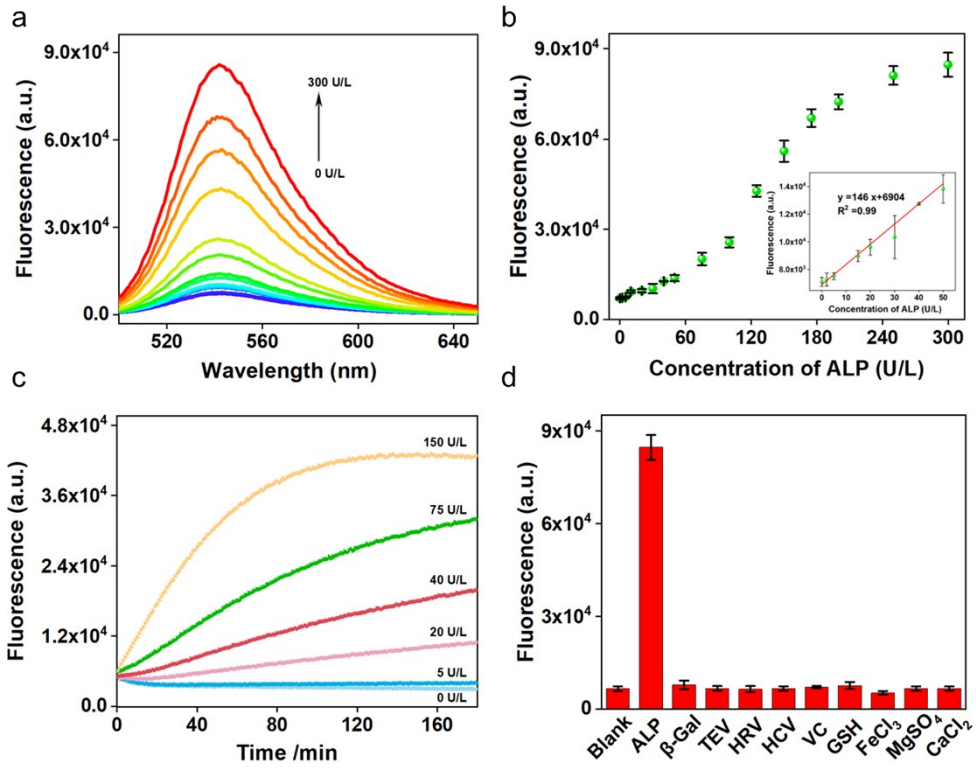

Fig. S24 (a) Fluorescence spectra of the FAST:ALP-HMBR complex in the presence of different concentrations of ALP. (b) Fluorescence intensity of the FAST:ALP-HMBR complex vs. the concentration of ALP. (c) Kinetic analysis of ALP-srFAST in the presence of different concentrations of ALP. (d) Selectivity of ALP-srFAST to different compounds. The concentration of each compound is 1.0 mM.

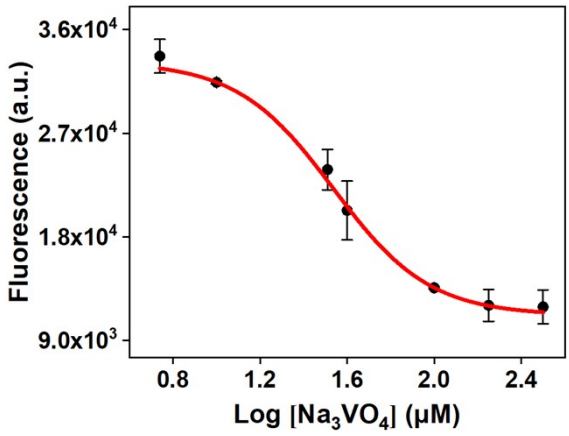

Fig. S25 The inhibition curve of Na_3VO_4 for ALP using ALP-srFAST. ALP (100 U/L) and Na_3VO_4 (different concentrations) were incubated in Tris-HCl buffer for 30 min, and then ALP-HMBR and FAST protein were added. The fluorescence of the mixture was recorded after 90 min.

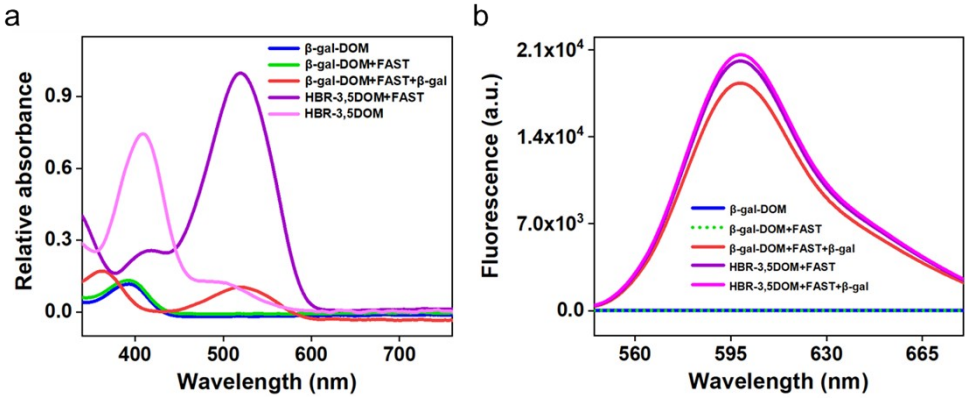

Fig. S26 (a) Absorption spectra of β-gal-DOM (blue), the FAST:β-gal-DOM complex (green), the FAST:β-gal-DOM complex reacted with β-gal for 60 min (red), the HBR-3,5DOM:FAST complex (purple) and HBR-3,5DOM (light magenta). (b) Fluorescence spectra of β-gal-DOM, β-gal-DOM + FAST ± β-gal and HBR-3,5DOM + FAST ± β-gal.

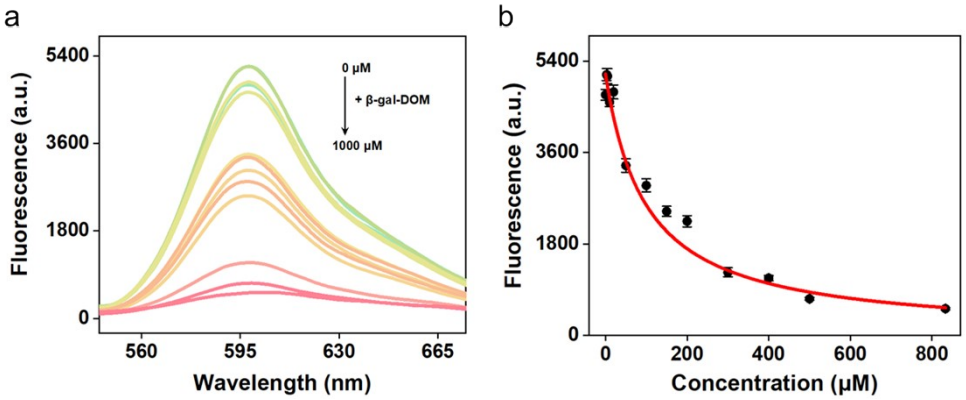

Fig. S27 (a) Fluorescence spectra of the competition assay between β-gal-DOM and HBR-3,5DOM. Different concentrations of β-gal-DOM were added to the solution containing 5 μM HBR-3,5DOM and 0.5 μM FAST. (b) The fluorescence intensity at equilibrium for various β-gal-DOM concentrations in the competition assay. K_d = 16.3 μM. λ_{ex} = 518 nm, λ_{em} = 600 nm.

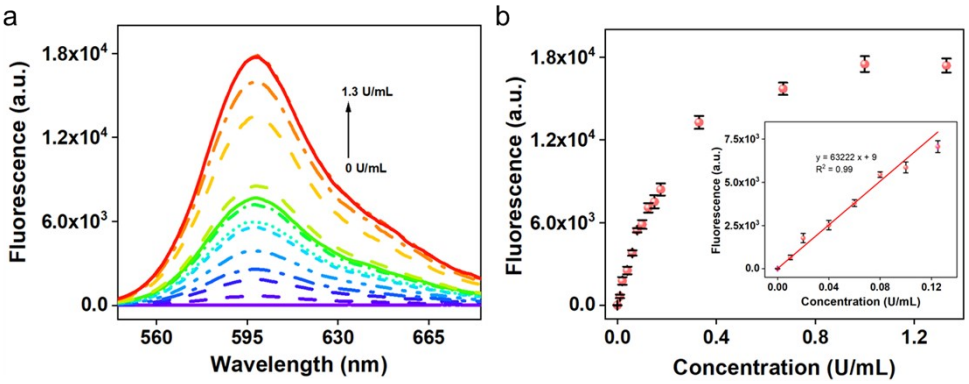

Fig. S28 (a) Fluorescence spectra of the FAST:β-gal-DOM complex in the presence of different concentrations of β-gal. (b) Fluorescence intensity of the FAST:β-gal-DOM complex vs. the concentration of β-gal.

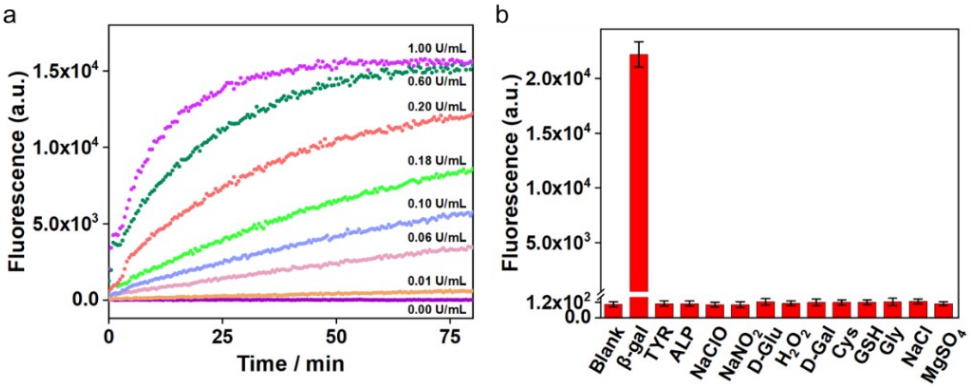

Fig. S29 (a) Kinetic analysis of β-gal-srFAST in the presence of different concentrations of β-gal. (b) Selectivity of β-gal-srFAST to different compounds. The concentration of each compound is 1.0 mM.

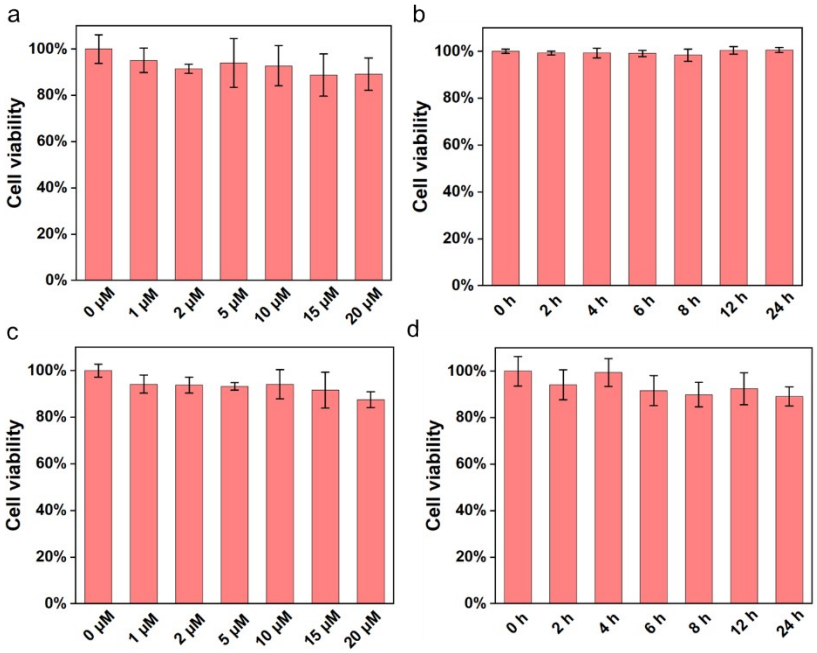

Fig. S30 Cell viability of HeLa (a, b) and SKOV-3 (c, d) cells measured by CCK8 assay. Effect of the ALP-HMBR concentration on viability of (a) HeLa and (c) SKOV-3 cells. The cells were incubated with different concentrations of ALP-HMBR for 6 h. Effect of the incubation time on viability of (b) HeLa and (d) SKOV-3 cells after being incubated with 5 μM ALP-HMBR for different times, respectively.

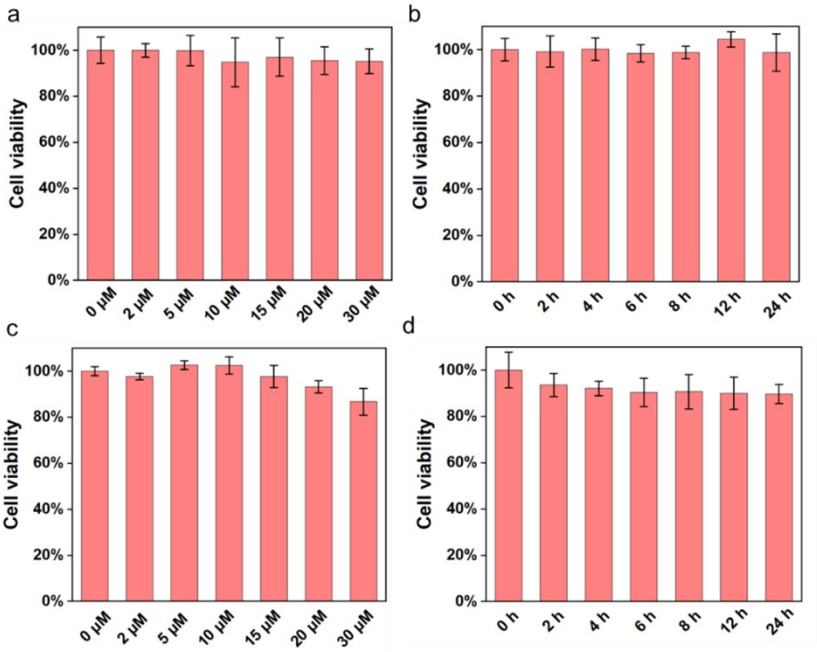

Fig. S31 Cell viability of HeLa (a, b) and SKOV-3 (c, d) cells measured by CCK8 assay. Effect of the β-gal-DOM concentration on viability of (a) HeLa and (c) SKOV-3 cell. The cells were

incubated with different concentrations of β-gal-DOM for 6 h. Effect of the incubation time on viability of (b) HeLa and (d) SKOV-3 cells after being incubated with 5 μM β-gal-DOM for different times, respectively.

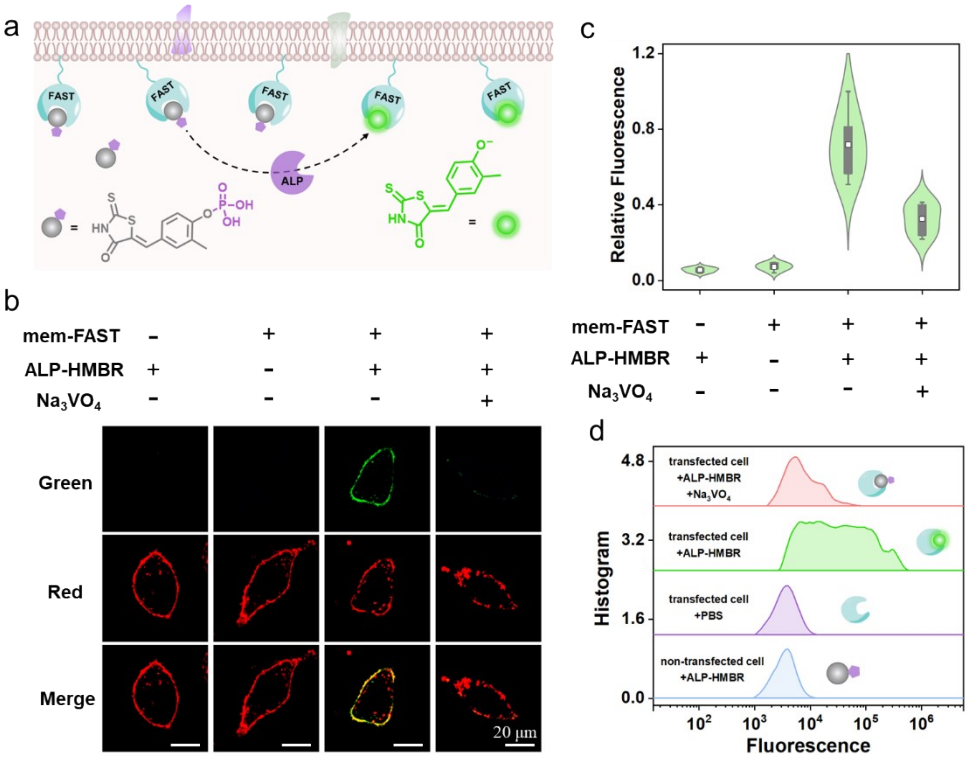

Fig. S32 ALP-srFAST for labeling of cell membrane. (a) Schematic of ALP-srFAST for labeling cell membrane of HeLa over-expressing ALP. (b) CLSM images of HeLa cells (transfected without or with pcDNA3.1-*mem-fast* for 24 h) treated with different conditions. The cells were incubated with DiI for 30 min firstly, and then were incubated with 5 μM ALP-HMBR for 90 min or Na_3VO_4 (400 μM, an inhibitor of ALP) for 30 min before being incubated with ALP-HMBR. The green fluorescence is from the FAST:HMBR complex, and the red fluorescence indicates the signals from DiI. (c) Quantification of the corresponding cells. Data are presented as the mean ± s.e.m. from 10 independent cells. (d) Flow cytometric analysis of HeLa cells under different conditions.

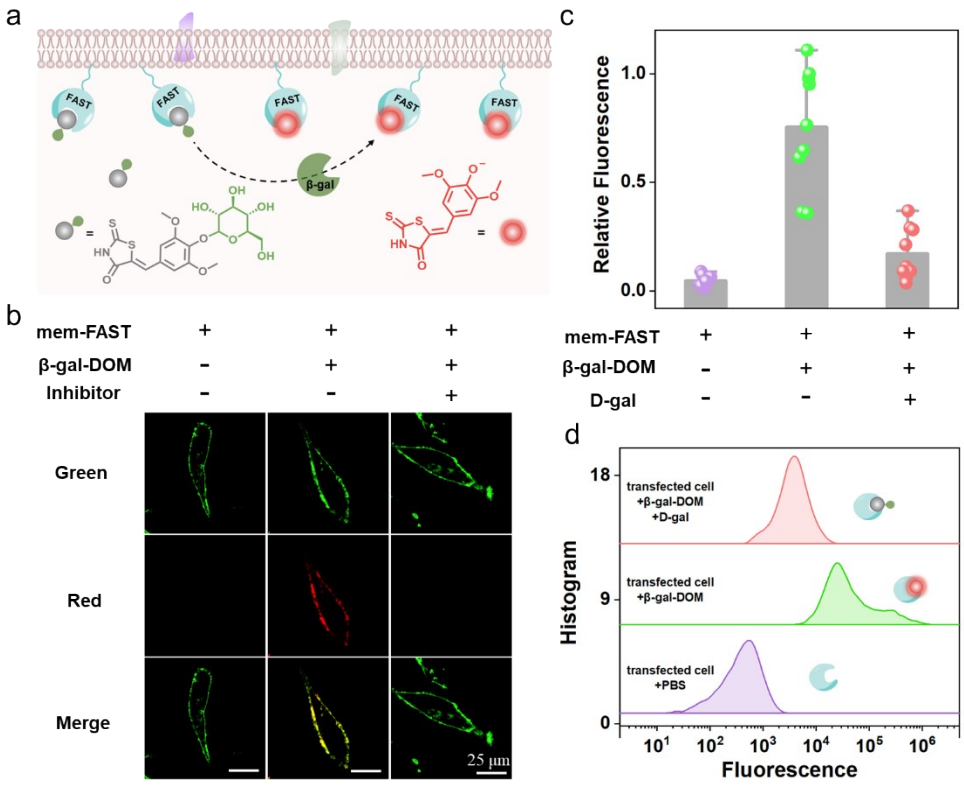

Fig. S33 β-gal-srFAST for labeling of cell membrane. (a) Schematic of β-gal-srFAST for labeling cell membrane of SKOV-3 cells over-expressing β-gal. (b) CLSM images of SKOV-3 cells (transfected with pcDNA3.1-*mem-fast* for 24 h) treated with different conditions. The cells were incubated with 5 μM HMBR + 5 μM β-gal-DOM for 90 min or D-galactose (1 mM, the inhibitor of β-gal) for 30 min before being incubated with HMBR and β-gal-DOM. The green fluorescence is from the FAST:HMBR complex, and the red fluorescence indicates the signals from the FAST:β-gal-DOM complex. (c) Quantification of the corresponding cells. Data are presented as the mean ± s.e.m. from 10 independent cells. (d) Flow cytometric analysis of SKOV-3 cells under different conditions.

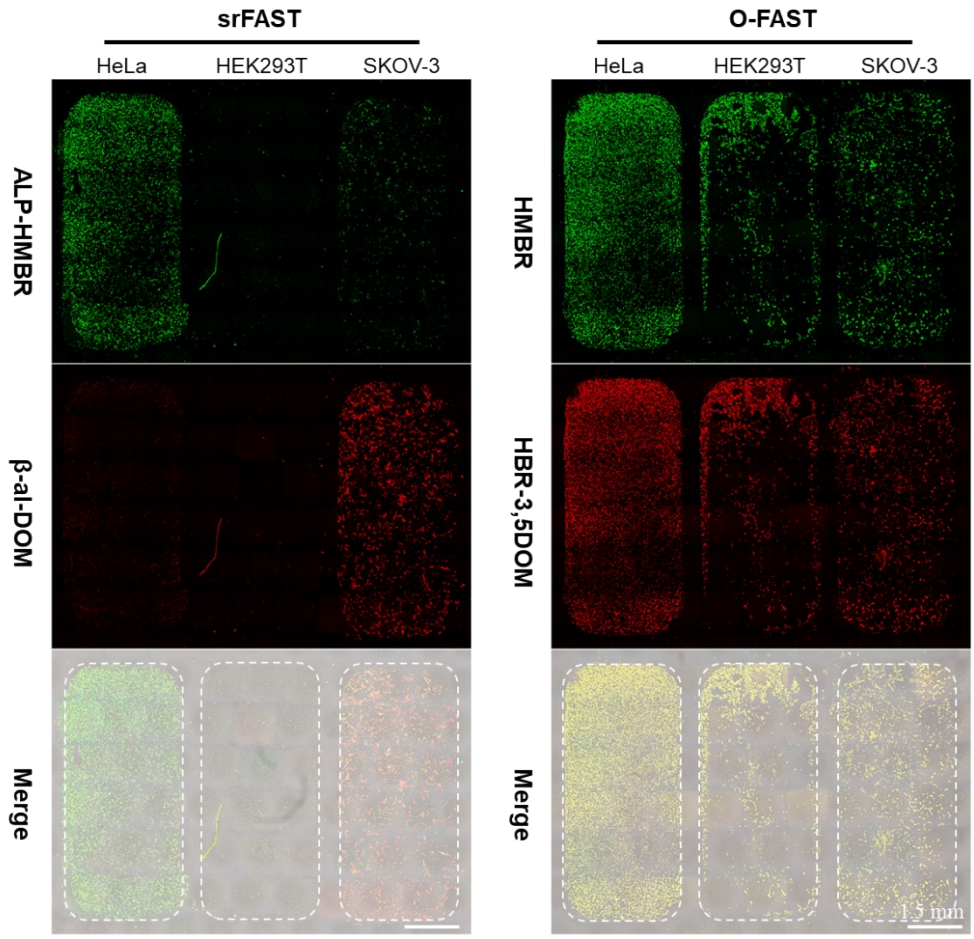

Fig. S34 Application of multicolor enzyme-srFASTs and O-FAST for selective labeling of cell membrane of the co-cultured cells. Mosaic images of the contiguous fluorescence imaging of the co-cultured cells.

4. NMR spectra

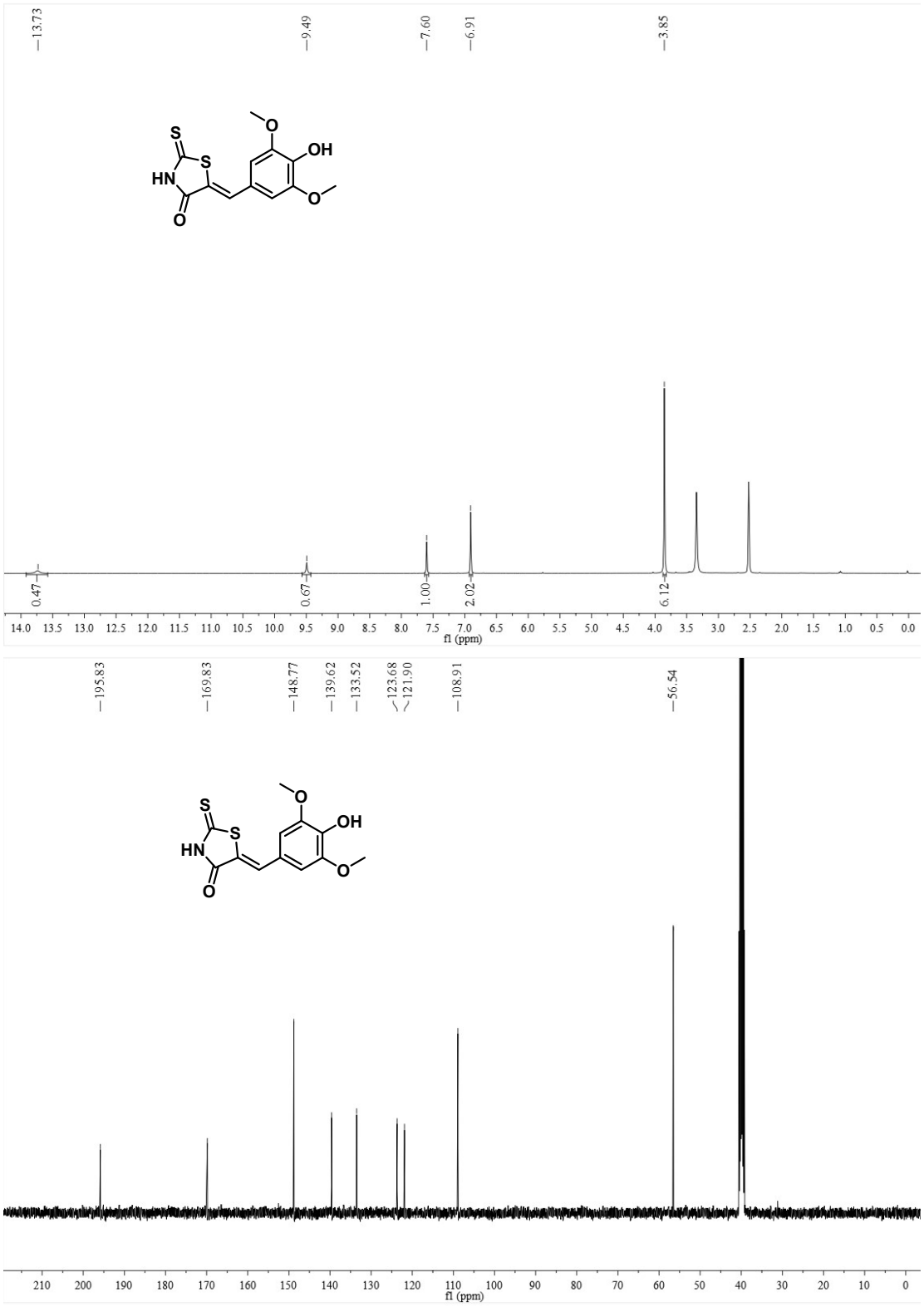

^{1}H NMR and ^{13}C NMR spectrum of HBR-3,5DOM in DMSO-d_6.

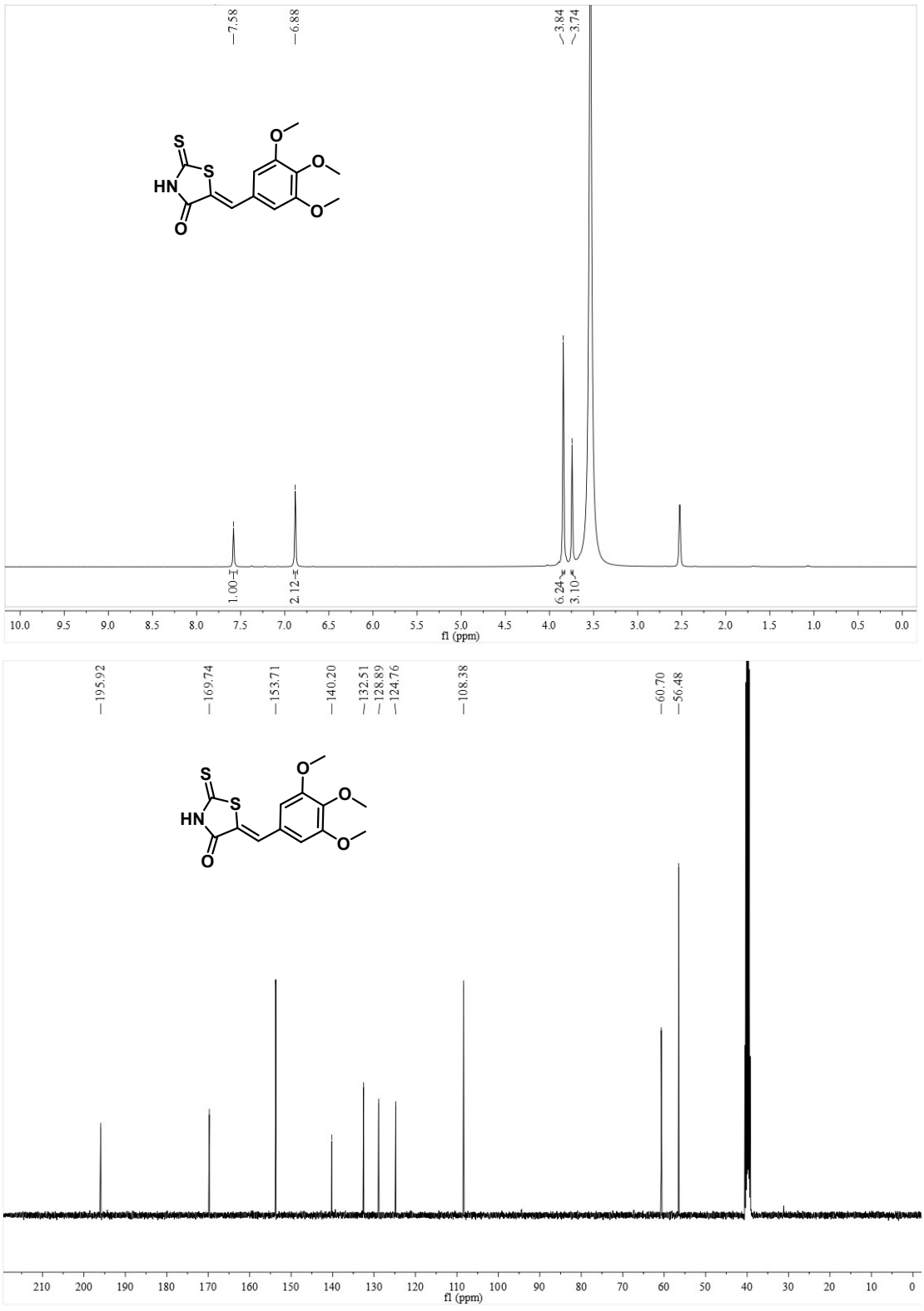

^{1}H NMR and ^{13}C NMR spectrum of HBR-3,4,5TOM in DMSO-d_6.

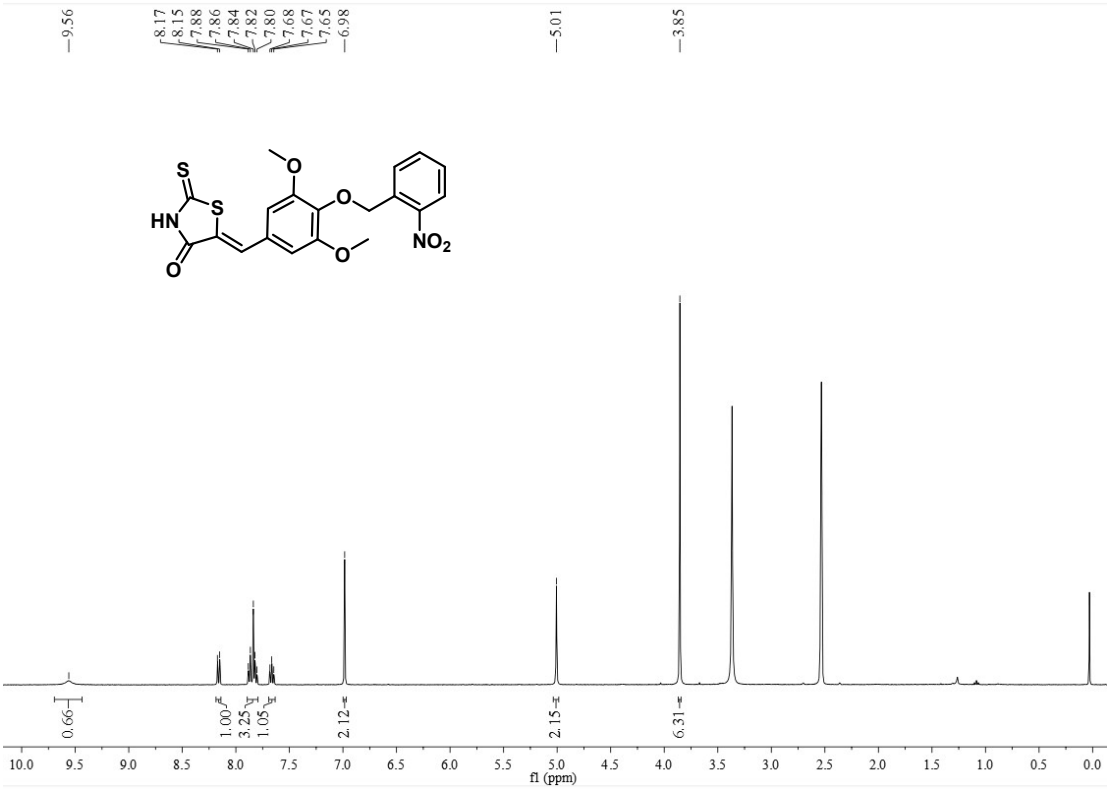

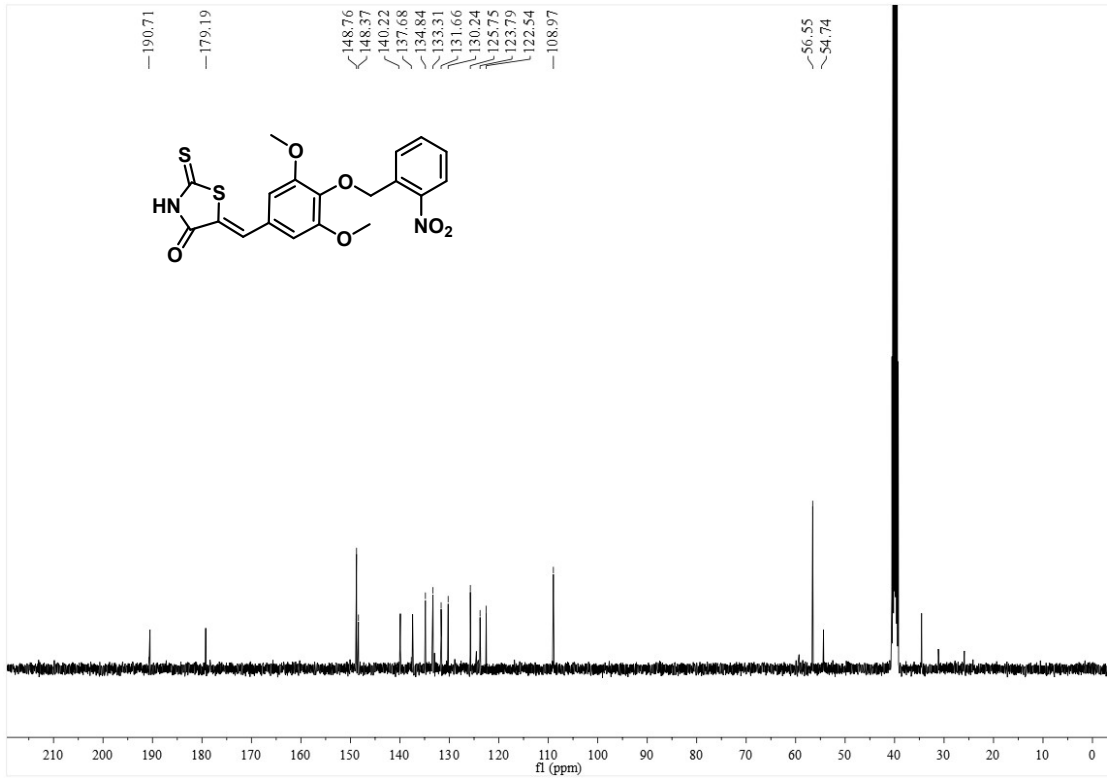

^{1}H NMR and ^{13}C NMR spectrum of photo-DOM in DMSO-d_6.

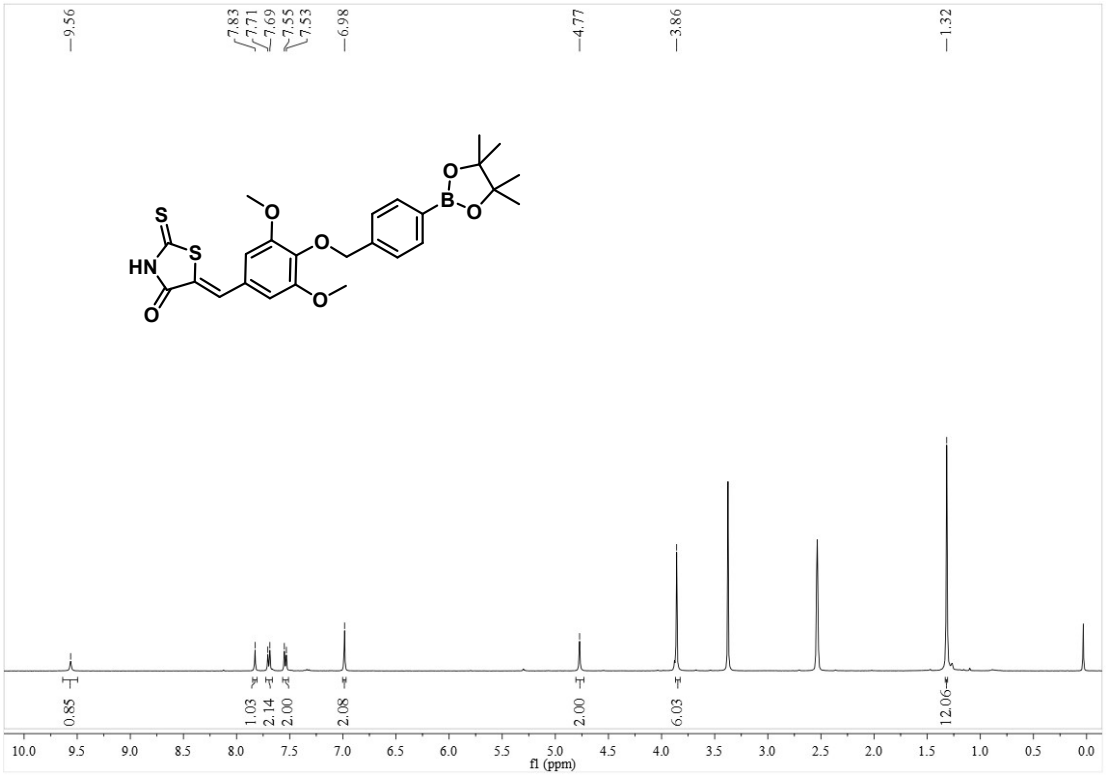

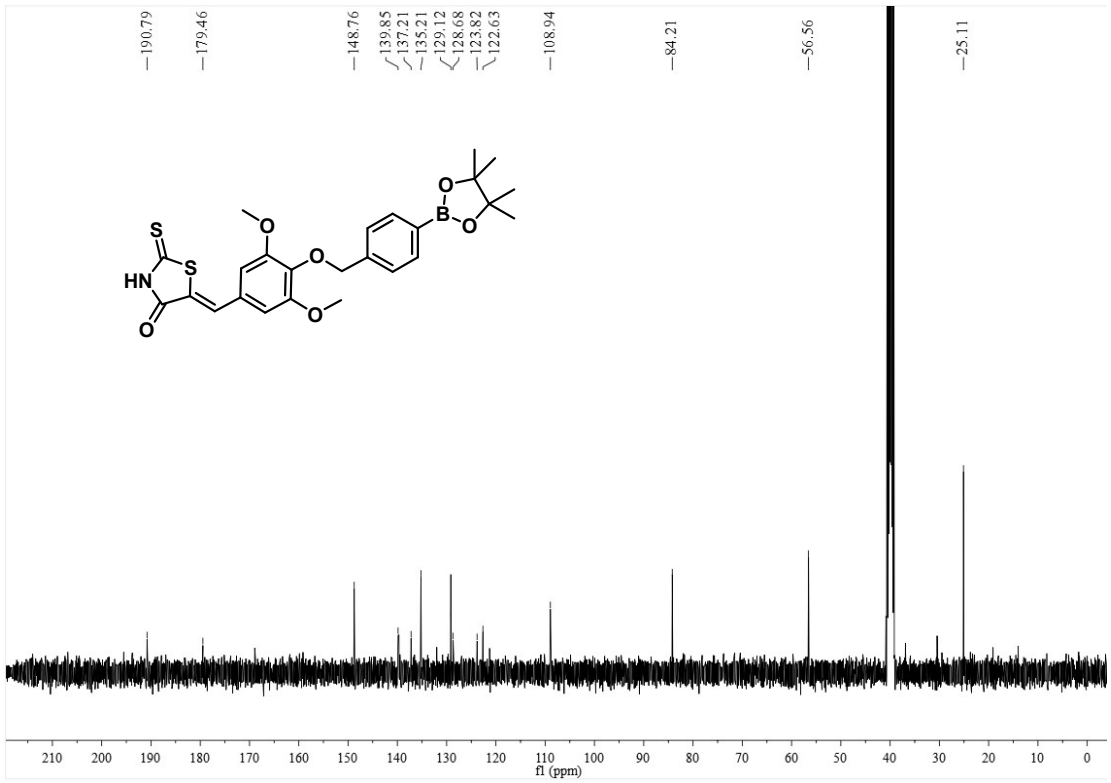

^{1}H NMR and ^{13}C NMR spectrum of H_2O_2-DOM in DMSO-d_6.

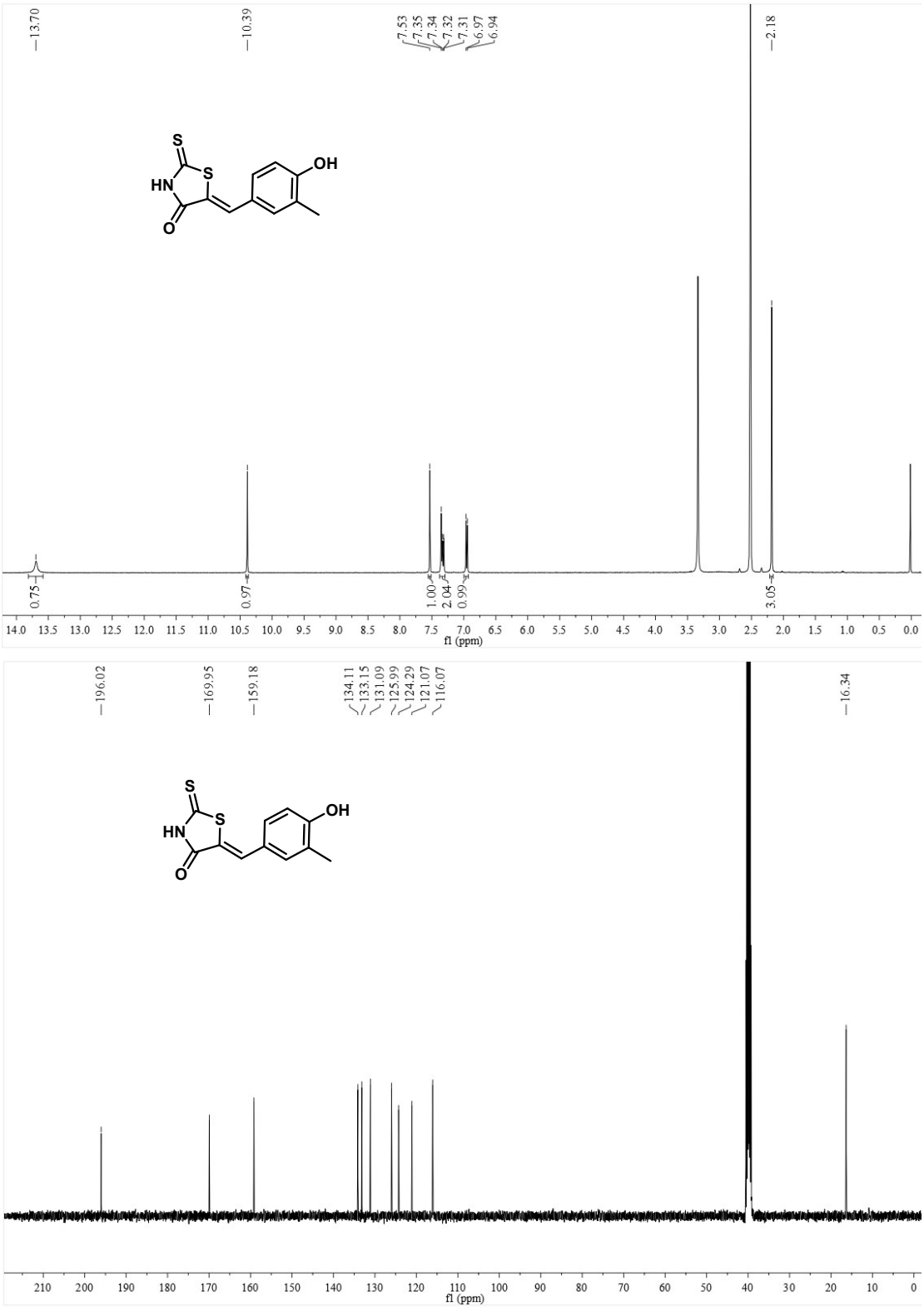

^{1}H NMR and ^{13}C NMR spectrum of HMBR in DMSO-d_6.

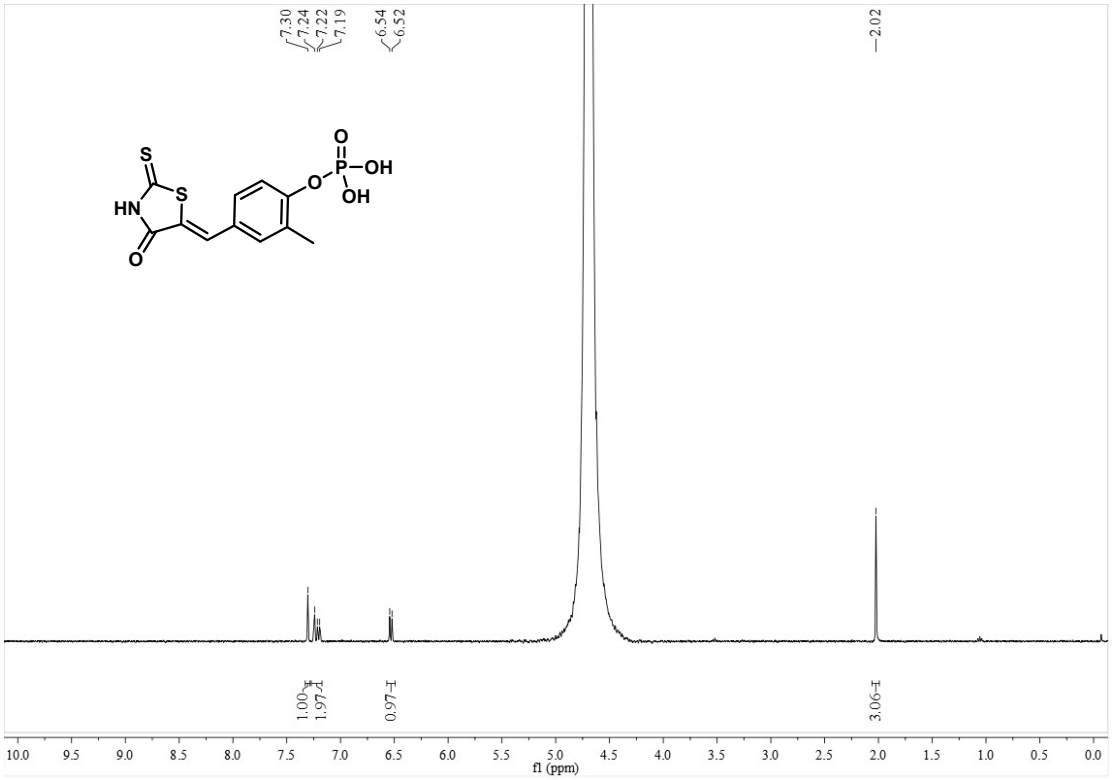

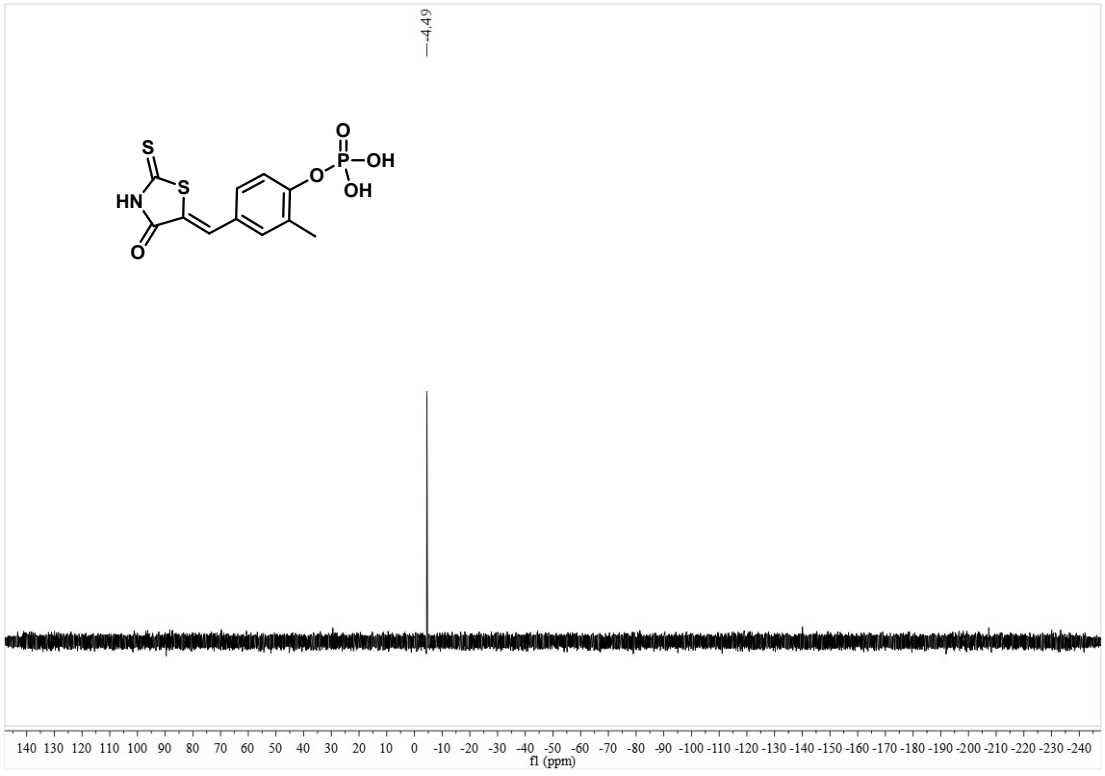

^{1}H NMR and ^{31}P NMR spectrum of ALP-HMBR in D_2O.

5. Mass spectra

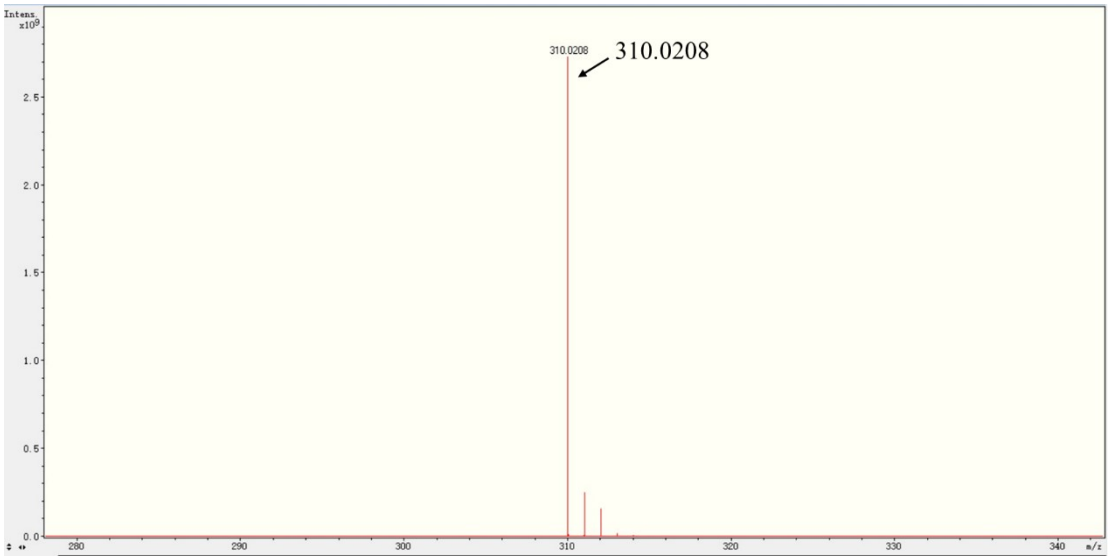

ESI-MS spectrum of **HBR-3,4,5TOM**

MS (ESI): m/z $[M-H]^-$ = calcd. for $C_{13}H_{12}NO_4S_2^-$ 310.0213; found 310.0208.

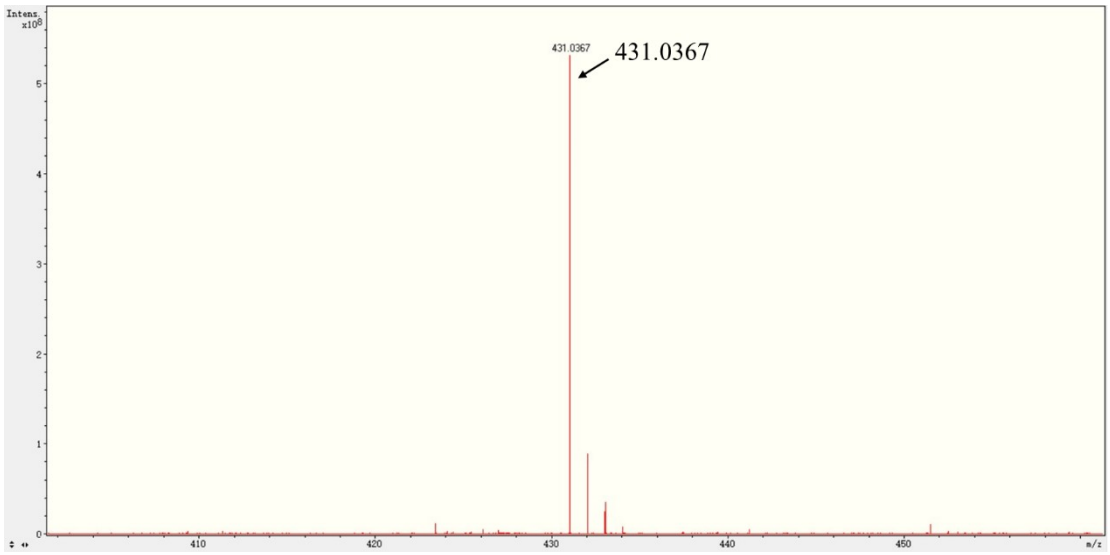

ESI-MS spectrum of **photo-DOM**

MS (ESI): m/z $[M-H]^-$ = calcd for $C_{19}H_{15}N_2O_6S_2^-$ 431.0377; found 431.0367.

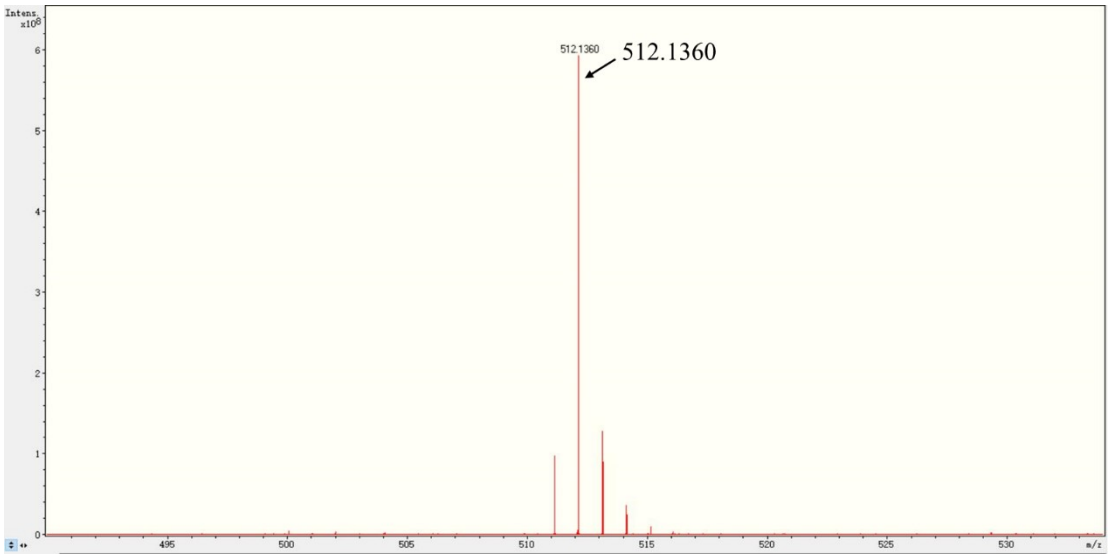

ESI-MS spectrum of **H_2O_2-DOM**

MS (ESI): m/z $[M-H]^-$ = calcd. for $C_{25}H_{27}BNO_6S_2^-$ 512.1378; found 512.1360.

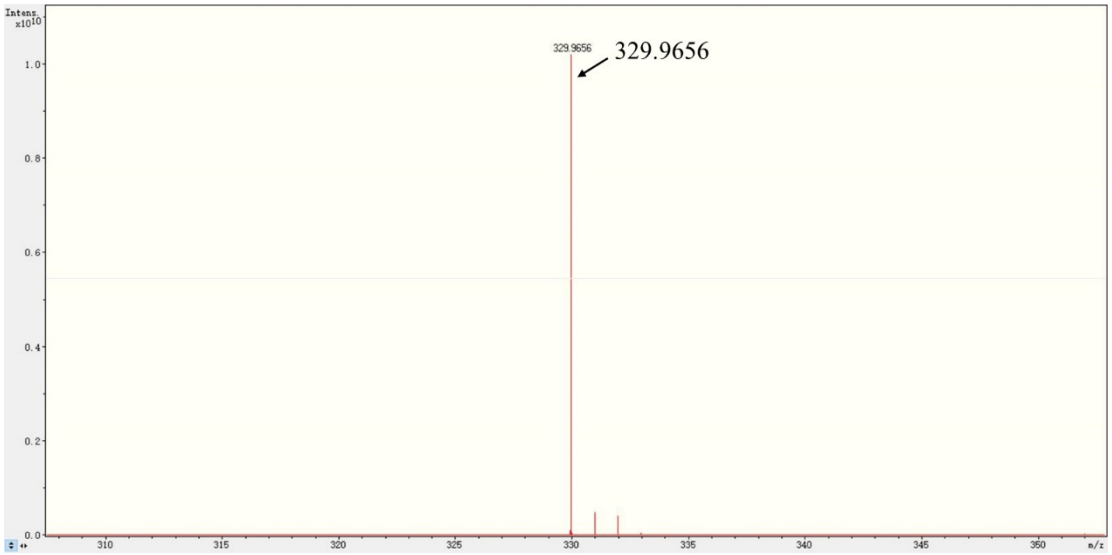

ESI-MS spectrum of **ALP-HMBR**

MS (ESI): m/z $[M-H]^-$ = calcd. for $C_{11}H_9NO_5PS_2^-$ 329.9665; found 329.9656.

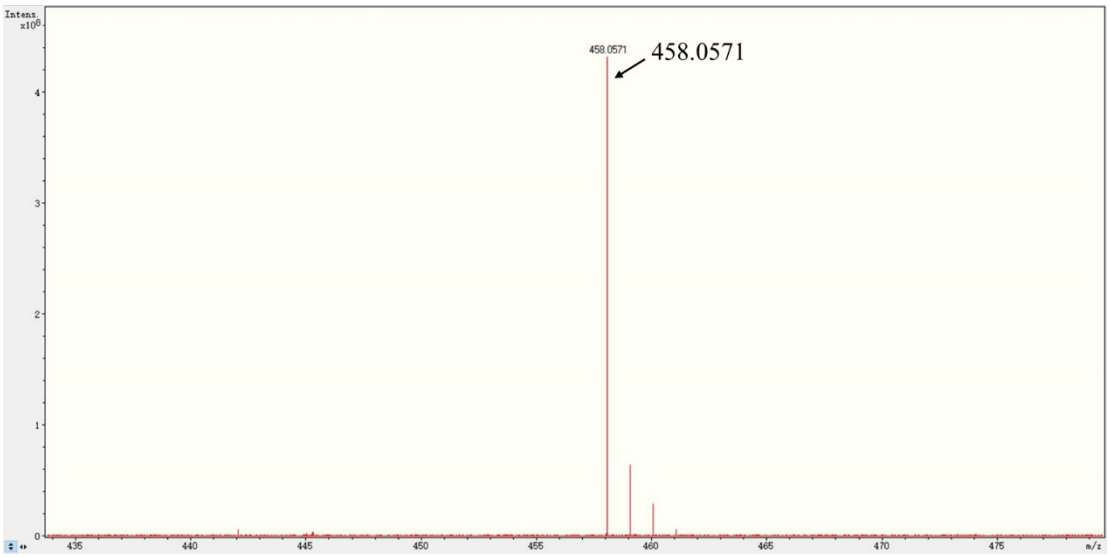

ESI-MS spectrum of **β-gal-DOM**

MS (ESI): m/z $[M-H]^-$ = calcd. for $C_{18}H_{20}NO_9S_2^-$ 458.0585; found 458.0571.

6. References

1. E. Runge and E. K. U. Gross, *Phys. Rev. Lett.*, 1984, **52**, 997-1000.
2. J. H. Zhang, H. Y. Li, B. Lin, X. Y. Luo, P. Yin, T. Yi, B. B. Xue, X. L. Zhang, H. Z. Zhu and Z. Nie, *J. Am. Chem. Soc.*, 2021, **143**, 19317-19329.
3. M. A. Plamont, E. Billon-Denis, S. Maurin, C. Gauron, F. M. Pimenta, C. G. Specht, J. Shi, J. Quérard, B. Pan, J. Rossignol, K. Moncoq, N. Morellet, M. Volovitch, E. Lescop, Y. Chen, A. Triller, S. Vriz, T. Le Saux, L. Jullien and A. Gautier, *Proc. Natl. Acad. Sci U.S.A.*, 2016, **113**, 497-502.
4. N. V. Povarova, S. O. Zaitseva, N. S. Baleeva, A. Y. Smirnov, I. N. Myasnyanko, M. B. Zagudaylova, N. G. Bozhanova, D. A. Gorbachev, K. K. Malyshevskaya, A. S. Gavrikov, A. S. Mishin and M. S. Baranov, *Chem. Eur. J.*, 2019, **25**, 9592-9596.